Genomics 113 (2021) 1349–1365

Contents lists available at ScienceDirect

Genomics

journal homepage: www.elsevier.com/locate/ygeno

Original Article

Evidence for discrete modes of *YAP1* signaling via mRNA splice isoforms in development and diseases

Jan Vrbský [a,*], Vladimir Vinarský [a,b], Ana Rubina Perestrelo [a], Jorge Oliver De La Cruz [a,b], Fabiana Martino [a,b,c], Antonio Pompeiano [a], Valerio Izzi [d,e], Ota Hlinomaz [a], Vladimir Rotrekl [c], Marius Sudol [f,g,h], Stefania Pagliari [a], Giancarlo Forte [a,b,*]

[a] International Clinical Research Center (ICRC), St Anne's University Hospital, CZ-65691 Brno, Czech Republic
[b] Competence Center for Mechanobiology in Regenerative Medicine, INTERREG ATCZ133, CZ-62500 Brno, Czech Republic
[c] Department of Biology, Masaryk University, CZ-62500 Brno, Czech Republic
[d] University of Oulu, FI-90014 Oulu, Finland
[e] Finnish Cancer Institute, 00130 Helsinki, Finland
[f] Department of Physiology, Yong Loo Li School of Medicine, Block MD9, 2 Medical Drive #04-01, 117597, Singapore
[g] Mechanobiology Institute, T-Lab, 5A Engineering Drive 1, 117411, Singapore
[h] Department of Medicine, Icahn School of Medicine at Mount Sinai, NY, New York 10029, United States of America

ARTICLE INFO

Keywords:
YAP1 isoforms
Alternative splicing
Tissue-specific expression
Cardiac differentiation

ABSTRACT

Yes-associated protein 1 (YAP1) is a transcriptional co-activator downstream of Hippo pathway. The pathway exerts crucial roles in organogenesis and its dysregulation is associated with the spreading of different cancer types. YAP1 gene encodes for multiple protein isoforms, whose specific functions are not well defined. We demonstrate the splicing of isoform-specific mRNAs is controlled in a stage- and tissue-specific fashion. We designed expression vectors encoding for the most-represented isoforms of YAP1 with either one or two WW domains and studied their specific signaling activities in YAP1 knock-out cell lines. YAP1 isoforms display both common and unique functions and activate distinct transcriptional programs, as the result of their unique protein interactomes. By generating TEAD-based transcriptional reporter cell lines, we demonstrate individual YAP1 isoforms display unique effects on cell proliferation and differentiation. Finally, we illustrate the complexity of the regulation of Hippo-YAP1 effector in physiological and in pathological conditions of the heart.

1. Introduction

Yes-Associated Protein 1 (YAP1) is one of the two main downstream effectors of the Hippo tumor suppressor pathway in mammals, a signaling pathway found to be crucial in the regulation of numerous biological processes, beyond cancer '*per se*' [47,57]. YAP1 functions are mainly related to the regulation of cell growth, proliferation [5,66,72], stemness [70,75] and differentiation [34,37], and recently YAP1 was also found regulating the immune system [77]. Its aberrant activation has been shown to contribute to tumor cell proliferation and cancer metastasis [7,10,35,46].

Independently of empirical results, the signaling function of the YAP1 protein could be theoretically deduced from the presence of modular and functional domains within its structure, namely the TEAD-interaction domain (TID) and either one or two WW domains ([67, 33, 4]). In addition, the YAP1 protein harbors a Src Homology 3 (SH3) protein-protein interaction-binding motif and a transcriptional Trans-Activating-Domain (TAD), which contains coiled-coil region [60,67]. The very carboxy- (C) terminus of YAP1 contains the PDZ domain-binding motif that is one of its two nuclear localization signal sequences [29,59]. When the Hippo pathway is "off", YAP1 with the deleted PDZ domain-binding motif, comprised of the 5C-terminal amino acids, does not translocate to the cell nucleus, when compared with the wild type YAP1 [44]. Importantly, the coiled-coil region of YAP1 was recently shown to mediate the formation of heterodimer complexes with TAZ protein, the paralogue of YAP1 [3]. This finding has wide ramifications for our understanding of how YAP1 isoform proteins signal when their coiled-coil regions are disrupted via differential splicing.

In general, the presence of structured domains and their cognate peptide motifs that mediate protein-to-protein interactions within

* Corresponding authors at: International Clinical Research Center (ICRC), St Anne's University Hospital, CZ-65691 Brno, Czech Republic.
E-mail addresses: jan.vrbsky@fnusa.cz (J. Vrbský), giancarlo.forte@fnusa.cz (G. Forte).

https://doi.org/10.1016/j.ygeno.2021.03.009
Received 1 November 2020; Received in revised form 10 February 2021; Accepted 5 March 2021
Available online 11 March 2021

selected signaling proteins imply a possibility of vast repertoires of combinatorial, multi-component complexes that ultimately could orchestrate precise signaling "out-puts" [49,61]. Following the activation of Hippo pathway upstream kinases MST and LATS by cell-to-cell contacts, YAP1 is phosphorylated at various Serine (S) residues, including S109, S127, S164 [73], with the decoration of the S127 by phosphate being the dominant regulatory switch [2]. The phospho-S127 YAP1 protein is retained in the cytoplasm where it cannot exert its co-transcriptional function. The regulation of YAP1 function by the Hippo pathway has been comprehensively reviewed (e.g.; [18,52,62]).

An additional level of signaling complexity stems from the existence of numerous YAP1 isoforms that are generated as a result of alternative mRNA splicing [17,56,63]. In *Drosophila*, only four Yki (fly orthologue of YAP1) isoforms were described so far, while three were found in the silkworm [35]. Six isoforms were predicted to exist in mouse (UniProtKB - P46938), and eight coding splicing variants, which were also detected as transcripts in cells, were so far characterized in human cells [17]. The main differences among hYAP1 isoforms include the usage of exon four, which is the exon that encodes the entire second WW domain, and the presence of the terminal part of exon five together with exon six, both of which are embedded within, and disrupt, the coding region for the Leucine zipper sequence-motif [17].

Based on their sequences and inferred structures, the YAP1 isoforms could be predicted to have unique protein interactors and thus to possibly exert slightly different, if not unique, functions. Therefore, we decided to examine all the published results, especially those in which measurements of total YAP1 expression and activity were performed in organs or cell types in which YAP1 isoforms might be, or likely are, differentially expressed.

For example, YAP1 activity as an oncogene was defined by describing the interaction of isoform hYAP1-2γ with PTPN14 (Liu et al. 2013 [55]). Similarly, YAP1 effects on cellular proliferation and protection from apoptosis were reported upon the overexpression of the same isoform *in vitro* [20]. Instead, a reduced proliferation and the concomitant increase in cell death in the squamous cell carcinoma line were detected when isoform hYAP1-2α was expressed [12]. Interestingly, few studies reported that differences in YAP1 isoform activity can be associated with the number of WW domains. The number of WW domains defining YAP1-1 and YAP1-2 isoforms was shown to be crucial in the promotion of cell apoptosis, in serum-starved cells, as measured by PARP cleavage and p73 stabilization [43]. Similarly, hYAP1-2α has been reported as a stronger co-transcriptional activator for the carboxyl-terminal fragment of ErbB-4 as compared to hYAP1-1β [30]. Apart from the functional differences ascribed to the number of WW domains, other regions of the YAP1 gene, namely the Leucine zipper that mediates heterodimers with TAZ, was shown to be important for the activity. YAP1 isoforms, mainly γ and δ isoforms that have compromised the canonical Leucine zipper motif, exhibited a dramatically reduced co-activator function [14,15].

Also, differences in the induction of TAZ protein degradation was described by using three YAP1 isoforms (hYAP1-2α, hYAP1-1α, and hYAP1-1β), as documented in HeLa and D645 cells [14].

It was also shown that mouse Shp2 phosphatase protein interacted with the shorter form of YAP1, known as YAP1-2α, but not with the longer form of YAP1, known as YAP1-2γ, confirming that YAP1 isoforms indeed have the ability to assemble different signaling complexes [65].

Intriguingly, YAP1 isoforms with disrupted Leucine zippers showed strong pro-oncogenic activity in cell culture models but when the tumorigenicity was tested in mice, it was YAP1-2α isoform with the intact Leucine zipper that induced much larger tumors than those driven by the expression of YAP1-2γ isoform with compromised Leucine zipper [3].

YAP1 also plays a key role during the development and differentiation of muscle satellite cells (Judson et al., 2012 [58]), in neural cell differentiation (Zhang et al., 2012 [69]), mesoderm specification [13] and also in pancreatic β-cell differentiation (Rosado-[45]). Unfortunately, no information on the specific isoform involved was given in the studies.

Here, we describe how YAP1 splicing isoforms function depending on the cell type and their differentiation status and identify the isoform-specific interacting partners of YAP1 and their cumulative effects on the transcriptional activity of the YAP1-TEAD complex. We also demonstrate that YAP1 splicing variants elicit distinct abilities to trigger TEAD-mediated transcription, while displaying unique effects on cellular proliferation, differentiation, and on the process of mechano-transduction. Finally, we show that the expression of YAP1 isoforms is differentially regulated in human pathological heart, thus opening a possibility of using selected YAP1 transcripts as early markers, if not potential harbingers, of cardiovascular diseases.

2. Results

2.1. YAP1 RNA undergoes tissue-specific alternative splicing

Regardless of its participation in the development and homeostasis of many organs [5,21], the actual expression of YAP1 in different organs and tissues of the human body is still poorly understood. We, therefore, performed an unbiased bioinformatics analysis of available transcriptomic datasets to access the level of YAP1 expression within different tissues (Fig. 1a). The analysis revealed detectable levels of YAP1 mRNA in a plethora of organs and tissues, with the relatively highest level of expression in smooth muscle, followed by endometrium, urinary bladder, and ovary. Significant differences were found among different muscle tissues: YAP1 RNA levels in skeletal and heart muscle are half and three times lower, respectively, as compared to smooth muscle. Interestingly, YAP1 mRNA was generally poorly detectable in the nervous system (midbrain, cerebral cortex, hypothalamus, etc.) and was below the detection limit in all the blood cell types analyzed. The latter result of a very low expression of YAP1 in white blood cells confirmed well the original finding of non-detectable YAP1 mRNA expression in these cells [59]. In general, YAP1 is considered as a relatively low level but rather ubiquitously expressed gene, as implied from the "Genotype-Tissue Expression study" (GTEx) with an interval of median-read-count per base of *YAP1* gene up to 6.4 only and the RNA blot analysis of mammalian organs and tissues [59].

Human YAP1 pre-mRNA undergoes alternative splicing (AS), an event that results in the generation of coding and non-protein-coding isoforms. YAP1 isoforms in humans share a high level of sequence and structure similarities (Fig. 1b). This very fact makes the production of isoform-specific antibodies for YAP1 protein isoforms difficult and invites efforts to generate monoclonal antibodies to short epitopes. Our analysis of the main genome databases identified twelve annotated YAP1 transcripts (Table 1). Eight of them (YAP1-1α, YAP1-1β, YAP1-1γ, YAP1-1δ, YAP1-2α, YAP1-2β, YAP1-2γ, and YAP1-2δ) were identified and characterized in 2012, from which a standardized nomenclature was proposed in order to ensure comparability of published data from functional studies where cDNAs of several isoforms are being used [17,56,63]. An additional isoform - Isoform 4 (i4) resembles an N-terminally truncated YAP1-2γ containing an alternative first exon inside the canonical intron one. Two remaining isoforms (YAP-205 and YAP-206; Ensembl) do not encode for any protein and their existence is supported by single Expressed Sequence Tag (EST) only. Interestingly, neuron-specific YAP1 isoforms with deleted C-terminal regions were also reported in the developing mammalian brain. As a result of the use of several mini-exon sequences between the exon 5 and exon 6 of the gene, these isoforms encode C-terminally truncated YAP1 proteins [16,23].

In order to get an insight into YAP1 splicing regulation in different human tissues, we compared YAP1 exon usage through the Genotype-Tissue Expression project (GTEx). By visualizing the median read counts of YAP1 exons obtained in a number of tissues and cell types, we observed a proportional variability of the same exons in between

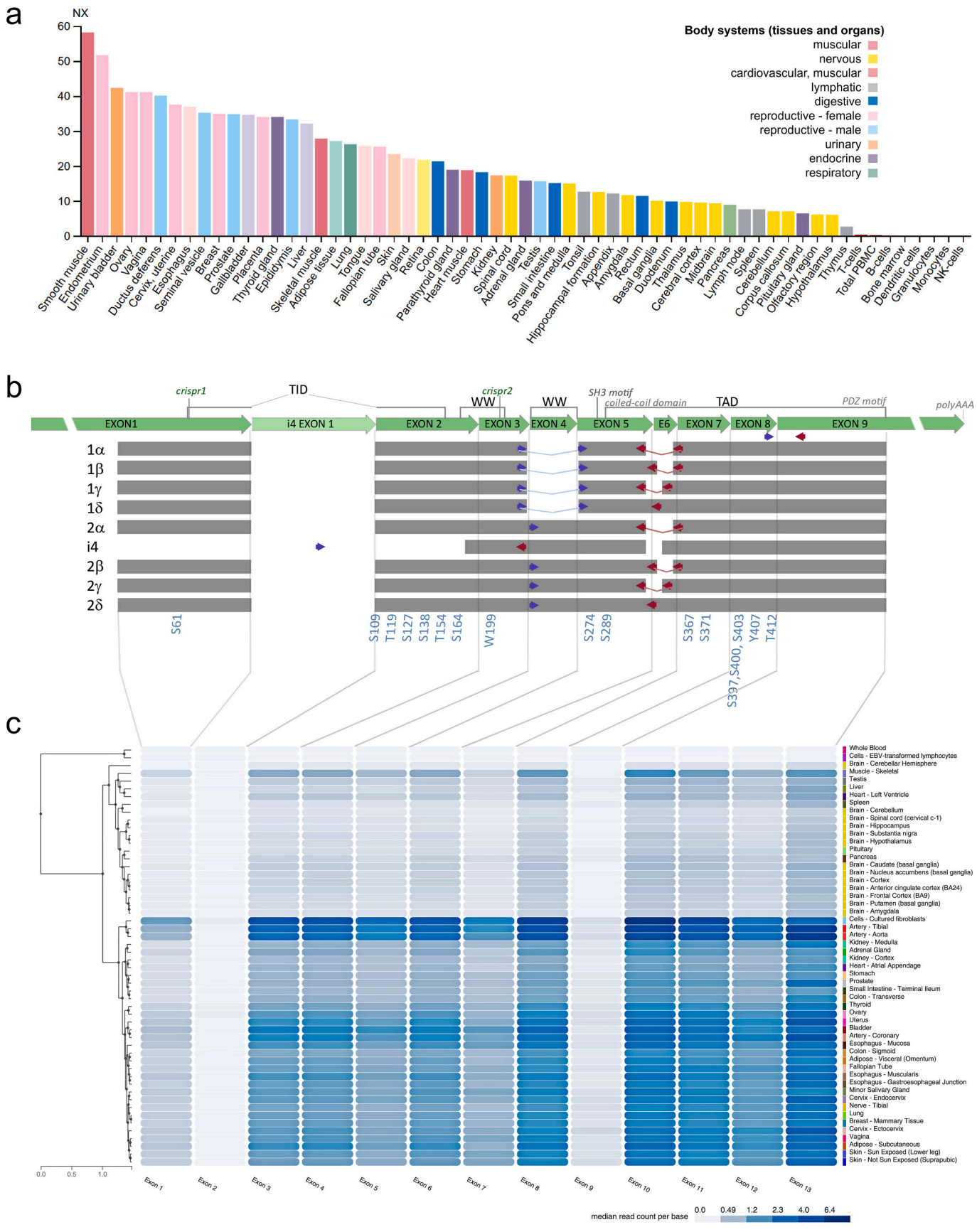

(caption on next page)

Fig. 1. Tissue-specific distribution of YAP1. (a) Tissue-specific expression of YAP1 RNA in 55 tissue types and 6 blood cell types represented as Consensus Normalized eXpression (NX) levels. The graph combines the data from three transcriptomics datasets (HPA, GTEx and FANTOM5). (b) Schematic representation of protein-coding YAP1 isoforms. Coding regions (CDS) of four YAP1-1, four YAP1-2, and YAP-i4 isoforms are aligned and corresponding protein domains (TEAD-binding domain (TBD), WW domains, TRANS-activating-domain (TID) with N-terminal coiled-coil domain and N terminal PDZ motif) are shown. Variability in splicing sites allows the design of isoform-specific primer pairs (blue- and red arrows). The location of main Serine (S), Tyrosine (Y) and Tryptophan (W) phosphorylation sites, some of which are known to be associated with YAP1 activity (S109, S127, S164, etc.), and W199, is indicated. (c) YAP1 EXON usage in human tissues shows proportional variability of thirteen YAP1 exons suggesting differences in YAP1 isoform expression. The 13 exons annotated in GTEx perfectly match 9 canonical exons (as schematized in panel b), while includes an alternative exon 1 (E1) of i4 isoform, and further includes and alternatively truncated canonical E9 at the C-terminus and thus recognizing additional 3 exons (E11, E12, and E13) in isoforms 2a, 1b, i4, and YAP1-207. These annotations within e9 are not experimentally supported yet. Adapted from the GTEx project. (For interpretation of the references to color in this figure legend, the reader is referred to the web version of this article.)

Table 1
Annotation of alternatively spliced isoforms of human YAP1 gene. The list of YAP1 isoforms is organized according to the recent proposals of nomenclature ([17], and [56,63]) and the accession codes used in other databases (Transcript Ensemble, Ensembl ID, GenBank name and NCBI accession) are indicated. Number of amino acids (aa) and the molecular weight (kDa) for each isoform are shown. Isoforms YAP1-203, −205, −206, −207 have not been experimentally characterized yet. YAP1-207 is an un-reviewed translated protein in Ensembl and in UniProtKB databases. YAP1-205 is a retained intron non-coding splicing isoform. YAP1-206 is a predicted non-coding LncRNA.

YAP1 isoform (Sudol)	Transcript Ensembl	GenBank name	Ensembl ID	NCBI accession	aa	kDa	Alternative C terminus
YAP1-2γ	YAP1-201	i1	ENST00000282441.10	NM_001130145.3	504	54,5	Full
YAP1-2δ	YAP1-210	i9	ENST00000615667.4	NM_001282101.1	508	54,9	Full
YAP1-1δ	YAP1-202	i7	ENST00000345877.6	NM_001282099.1	470	50,5	Full
YAP1-2β	YAP1-209	i8	ENST00000537274.5	NM_001282100.1	492	53,2	Full
YAP1-1α	YAP1-204	i5	ENST00000526343.5	NM_006106.5	450	48,3	
YAP1-2α	YAP1-208	i2	ENST00000531439.5	NM_001195044.2	488	52,7	Truncated
YAP1-1β	YAP1-211	i3	ENST00000629586.2	NM_001282098.2	454	48,8	Truncated
YAP1-1γ		i6		NM_001282097.2	466	50	
	YAP1-203	i4	ENST00000524575.5	NM_001195045.2	326	36,2	Truncated
	YAP1-207		ENST00000529029.1		258	28,6	Truncated
	YAP1-205		ENST00000526594.1				
	YAP1-206		ENST00000528834.1				

different biological locales (Fig. 1c). We cannot be sure if the heatmap reflects accurately the usage of exons 2 and 4, because of the RNA-seq amplification process that could generate quantitative artifacts by itself. Nonetheless, this evidence suggests that YAP1 mRNA undergoes a tissue-specific regulation by alternative splicing.

2.2. YAP1 splicing isoform relative expression correlates with cell maturation and identity

Based on our bioinformatics analysis suggesting that YAP1 exons are generated in a tissue-specific fashion *in vivo*, we designed a set of primers

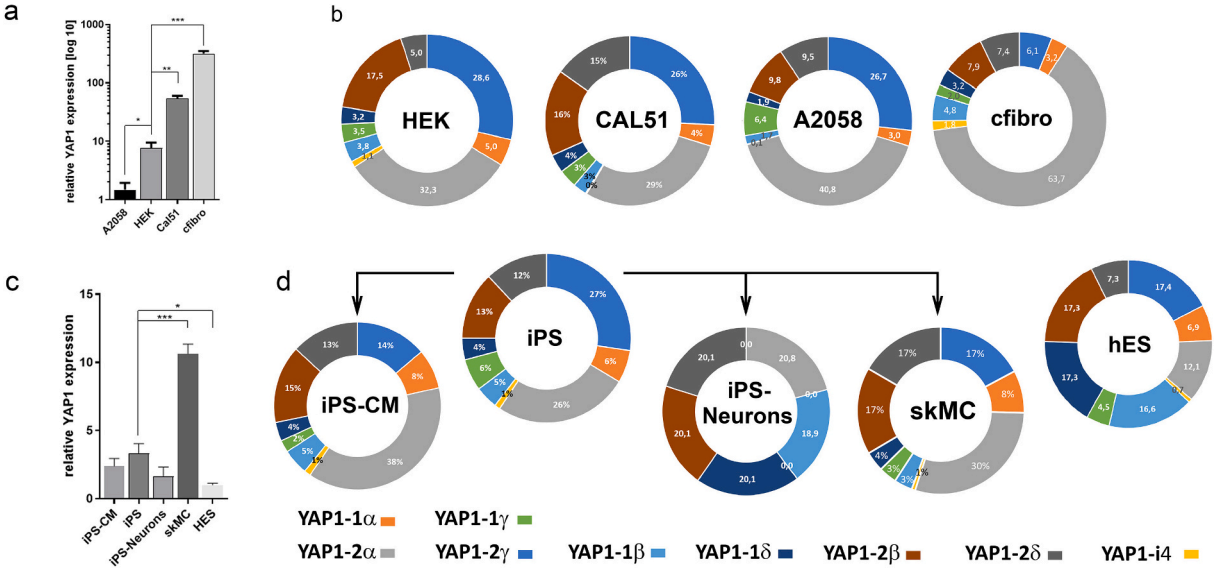

Fig. 2. YAP1 gene is differentially spliced in cells of different origin and during maturation. (a) Barplot quantification of relative total YAP1 expression in the indicated cell lines as obtained by RT-qPCR. The primers used were designed as to be complementary to conserved regions of YAP1. The data are relativized to YAP1 expression levels in A2058 cells and represent mean ± SEM, $n = 3$, one-way ANOVA. (b) Donut graph representation of the relative expression of YAP1 isoforms in human embryonic kidney (HEK H293), breast carcinoma line (CAL51), human metastatic melanoma (A2058), human cardiac fibroblasts (cfibros). The values for each indicated isoform are expressed as mean percentages. (c) Barplot quantification of total YAP1 expression relative to iPS cells. The data are represented as mean ± SEM, n = 3, one-way ANOVA (* 0,01 < $P \leq$0,05, ** 0,001 < P ≤0,01, *** P ≤0,001). (d) Donut graph representation of the relative expression of YAP1 isoforms in induced pluripotent stem cells (iPS), H9 human embryonic stem cells (hES), iPS-derived-cardiomyocytes (IPS-CM), −neurons (iPS-neurons) and -skeletal muscle cells (skMC). The values are expressed as mean percentages of the indicated isoform, $n = 3$.

suited to specifically recognize nine transcripts (see Fig. 1b and Materials and Methods section for details).

Thus, we performed RT-qPCR and calculated the relative levels of individual YAP1 protein-coding isoforms in selected human cell cultures that represented diverse cell types and pluripotency stages. Because YAP1 is known to be differentially expressed in normal and tumor cells, and its expression level was shown to correlate with tumor grade *in vivo* [42], we first tested YAP1 isoforms in human embryonic kidney cells (HEK293), cardiac fibroblasts (cfibros), triple-negative breast cancer (CAL51), and highly metastatic melanoma (A2058) cell lines. Overall, we found the *YAP1* gene to be expressed at significantly higher levels in cfibros, compared to other cells (215-fold vs. A2058, 41-fold vs. HEK293, 6-fold vs. CAL51) that we examined. However, among the tumor cell lines, CAL51 displayed the highest level as compared to HEK293, and A2058 (Fig. 2a).

The analysis of isoform abundance in the different cell types demonstrated that isoform 2α was the most represented transcript in all four cell types, with a percentage ranging from 29% in CAL51, to 32% in HEK293, 41% in A2058 and 64% in cfibros. Isoform 1β also appeared to be highly represented in most of the lines, with values ranging from 26% in the breast, to 29% in kidney and melanoma cells, while it only accounted for 6% of the total YAP1 in cfibros. The highest variability in the expression was found for the isoform 2β, which was consistently around 16–17% in CAL51 and HEK293 cells, while representing 10% of the total YAP1 RNA in A2058 metastatic line and 8% in cfibros. The levels of isoforms 1α, 1β, i4, 1γ, 2δ were consistently low in all four cell lines (Fig. 2b). This analysis suggested that YAP1 undergoes alternative splicing in a cell-type specific manner, and prompted us to ask whether this is also the case during development and in diseases.

To address this question, we analyzed the levels of YAP1 splicing variants in human embryonic (hES) and induced pluripotent stem cells (iPS), which are known to share numerous genetic similarities, while still representing distinct stages of pluripotency [19,41]. The analysis documented that hES express significantly lower levels of YAP1 transcript compared to iPS (Fig. 2c). Importantly, hES display rather different relative levels of individual isoforms and are characterized by the predominance of isoforms 2γ (27% vs. 17.4%) and 2α (26% vs. 12.1%) whereas the expression of isoform 1δ was much higher in hES (17.3%) compared to iPS (4%).

Next, we differentiated iPS towards cell types (i.e., lines) that were found to have an either high or low amount of YAP1 mRNA in our bioinformatics analysis (see Fig. 1a), assuming this variability might be reflected in isoforms distribution. We selected cardiac (iPS-CM) and skeletal muscle cells (iPS-skMC), or neuronal cells (iPS-neurons), and confirmed the differential expression of total YAP1 transcript in differentiated cells and iPS (Fig. 2c). Of interest, skeletal muscle cells expressed 6-times more YAP1 than cardiac muscle cells, thus confirming the transcriptomics data in Fig. 1. Next, we measured the relative abundance of YAP1 isoforms. Along with the progression of cell specification, we found the most significant changes in the decrease of 2γ relative expression in all three differentiation experiments (from 27% to 14% in iPS-CM, to 17% in iPS-skMC and 0% in iPS-neurons). Relative expression of 1γ isoform decreased analogously (from 6% to 2% in iPS-CM, to 3% in iPS-skMC and to 0% in iPS-neurons). Isoform 1δ was regulated differently: its expression increased during neuronal differentiation (from 4% to 20.1%), while staying at the same relative level in cardiomyocytes and skeletal muscle cells. In comparison, the relative expression of 2β, 2δ isoforms remained stable in all differentiated lines as compared to iPS cells (Fig. 2d). Altogether the expression of YAP1 isoforms was quite homogeneous between the skeletal and cardiac muscle cells as compared to the neural cells.

By comparing the expression of YAP1 isoforms, we found 2α, 2γ, 1β, and 2β respectively, to be the most abundant ones in the majority of the cell types tested. On the contrary, i4 was the least expressed isoform or its level was below the detection limit (i.e. in iPS-derived neurons).

Recently, YAP1 inactivation was proven crucial for pluripotent cell mesoderm specification and the subsequent acquisition of contractile phenotype [13]. We, thus, monitored the expression of YAP1 isoforms during cardiac maturation, up to the stage when contractile cardiomyocytes were clearly visible (day 8–16). The progression of iPS differentiation was confirmed in RT-qPCR by the loss of pluripotency marker NANOG and the acquisition of mesodermal markers EOMES, BRACHYURY, MESP1, MIXL1, followed by the increase of early (GATA4, Nkx-2.5) and late (MYL7, MYH7, TNNT2) cardiac markers (Fig. 3a). The analysis of YAP1 splicing variants expression showed an increase of all the isoforms during the first phase of cardiac induction, with a peak between day 4–8 (Fig. 3b), when cardiac progenitors are being formed, as documented by expression level of GATA4 and Nkx-2.5 markers. During the following phase, when contractile cardiomyocytes appeared (at around day 8), and continuing until day 16, the expression of all the isoforms decreased. Altogether, these data indicated that the alternative splicing of YAP1 occurs during cardiac differentiation. The levels of all isoforms display a similar trend, except i4 that remained low in all time points. Two most expressed isoforms in iPS cells (2α and 2γ) were also the most responsive, with increased fold change of approximately 4–5 during the early differentiation step, supporting their dominant role in cells with a different identity and during maturation.

The number of WW domains is deemed to be a crucial factor in determining YAP1 isoform activity [15,24,30,36,43,65].

In order to better understand whether the presence of one versus two copies of the WW domain could affect cardiac differentiation, we selected YAP1 isoforms with one (1α, 1γ) and with two (2α, 2γ) WW domains and cloned their coding sequences into expression vectors under the control of CAG promoter. The reading frame also contained an N-terminally-linked tdTomato fluorescent reporter by E2A sequence. Single isoforms were transfected into Troponin I1 reporter iPS line (TNNI-iPS) and the presence of the tomato transgene was monitored daily for the duration of 10–11 days. Cardiac differentiation was induced one-day post-transfection and the cells were cultured until spontaneous contraction could be seen and the morphologically well-defined TNNI-GFP-positive clusters of cardiac cells appeared. Consistent with our standardized protocol for *in vitro* cardiac differentiation, we were able to detect first contracting cardiomyocytes after 8 to 10 days of differentiation in all isoform-overexpressing cell cultures.

We enzymatically dissociated contractile areas and analyzed the concomitant expression of TNNI-GFP (cardiac differentiation marker) and tdTomato (YAP1 isoform expression) reporters in single cells by flow cytometry (Fig. 3c). While the over-expression of all four YAP1 isoforms displayed a tendency to reduce TNNI-GFP signal, the inhibitory effect was statistically significant only for YAP1-1α and 2γ isoforms. These results confirmed that YAP1 expression has an inhibitory effect on cardiac differentiation and suggests that YAP1-1α and -2γ isoforms might play a specific role in cardiac differentiation. Interestingly, the inhibitory activity of YAP1 was independent of the number of WW domains.

2.3. *YAP1 isoform splicing is differentially regulated in pathological heart*

YAP1 reactivation has been shown to occur in diseased heart tissue following myocardial infarction [8,39] and in failing heart, as a result of chronic, non-ischemic diseases [22]. This phenomenon has been described as “an attempt” to promote cardiomyocyte hypertrophy and survival, thus restoring organ functionality. Since cardiac diseases usually feature the substitution of portions of contractile with akinetic fibrotic tissue, we asked whether YAP1 isoform switch could be detected in the pathological heart.

We obtained human heart specimens from end-stage heart failure patients eligible for organ transplantation and as control we used non-transplantable hearts from deceased (healthy) donors. By Masson trichrome staining we confirmed the accumulation of fibrotic tissue in the pathological heart (Fig. 4a). Next, we analyzed the relative expression of YAP1 isoforms in different areas of the heart. We compared their relative

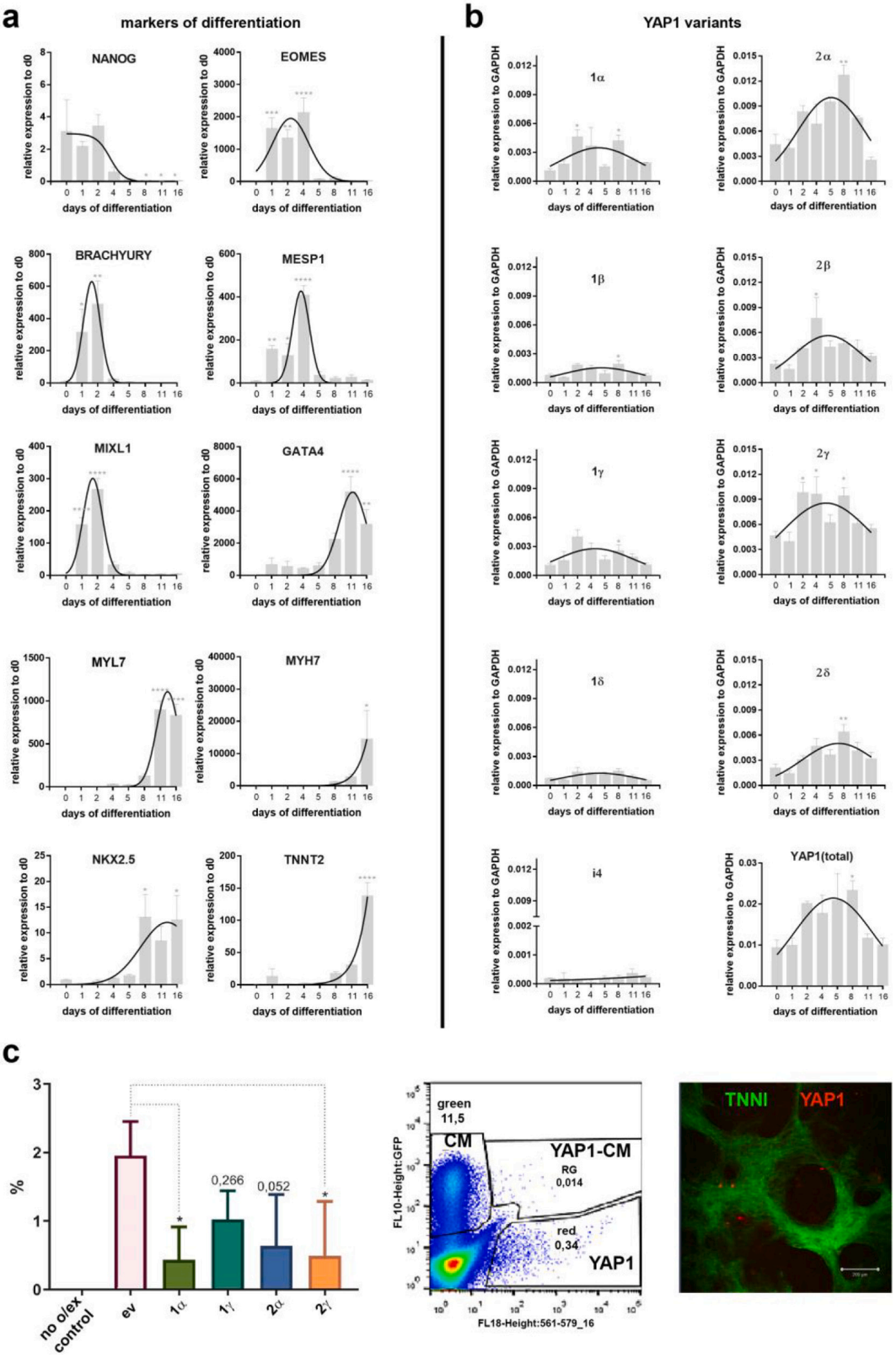

Fig. 3.

expression in healthy atria and ventricle and found that the most represented YAP1 isoform to be 1β, expressed at similar levels (40.6 to 43%) in both regions. However, the YAP1 isoform 2γ was more represented in the atria (22.5%) compared to the ventricle (3.8%), while 2δ had an opposite distribution (5.0 vs. 15.2%). These results suggest that the *YAP1* gene undergoes differential splicing in diverse regions of the heart, possibly reflecting the existence of specialized cell types in given locales (Fig. 4b).

Next, we investigated whether the balance among the isoforms was perturbed in the pathological heart. We, hence, analyzed the relative

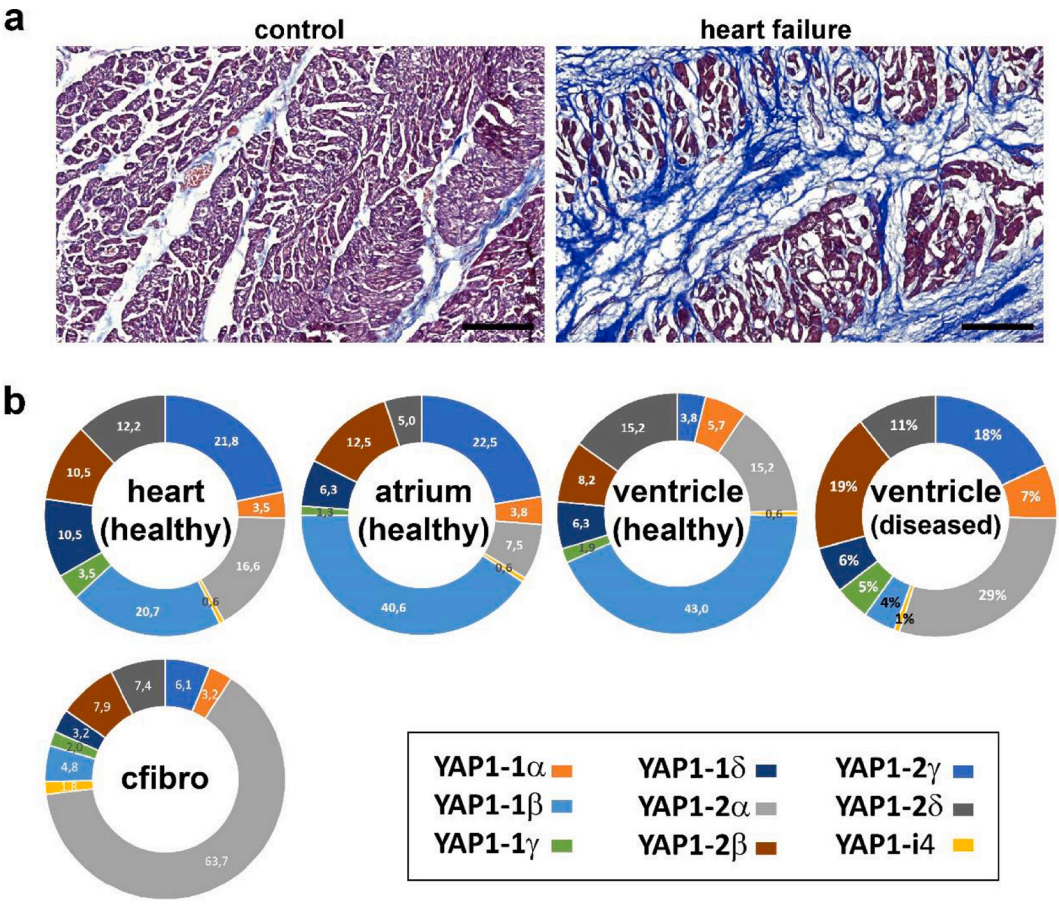

Fig. 4. Evidence for differential YAP1 gene splicing in pathological heart. (a) Representative image of Masson's trichrome staining of healthy (control, $n = 3$)) and pathological (heart failure, $n = 7$) human heart sections. Blue color indicates the accumulation of collagen fibers typical of the fibrotic tissue. The scale bar corresponds to 200 μm. (b) Donut plot representation (from 3 independent samples) of the relative expression profiles of YAP1 isoforms total healthy heart, healthy atrium, healthy and diseased ventricle, purified cardiac fibroblasts (cfibros). Data are expressed as mean percentages of YAP1 isoform RNA expression. The total RNA from human heart (Total Heart) was a pool from multiple hearts (Clontech, No. NC9900441). (For interpretation of the references to color in this figure legend, the reader is referred to the web version of this article.)

abundance of the isoforms in the ventricle of failing hearts from patients diagnosed with heart failure caused by hypertrophic cardiomyopathy. The results indicated that the pathological ventricle was characterized by a marked increase in 2α (29% vs. 15.2%) and 2β (19% vs. 8.2%), and the concomitant reduction in 1β (4% vs. 43%) isoforms. Since cardiomyocytes in the failing heart are substituted by fibrotic tissue and cardiac fibroblasts, we compared the relative expression of YAP1 isoforms in the pathological heart with cardiac fibroblasts that were obtained *ex vivo*. Similar to the diseased ventricle, cardiac fibroblasts displayed a predominance of isoform 2α (63.7%). This result suggested that the switch in YAP1 isoform composition in the pathological ventricle likely accounts for the increase in cardiac fibroblast presence in the pathological fibrotic tissue.

2.4. YAP1 isoforms engage differentially in TEAD-mediated transcription, display unique sensitivity to substrate stiffening and induce different proliferation responses

Members of the TEAD transcription factor family account for roughly 78% of YAP1-mediated transcription activity (Zanconato et al., 2015 [83]). YAP1-TEAD interaction is mediated via the amino-terminal region of YAP1, the TID domain [67] that is shared by all YAP1 isoforms except for YAP1-i4. To test whether splicing isoforms have a different ability to promote TEAD-mediated transcriptional activity, we transfected isoforms 1α, 1γ, 2α, or 2γ into 8xGTIIC-lux YAP1 −/− CAL51 lines [11,40]. Seventy-two hours after transfection, we quantified Luciferase activity in a TEAD-based "readout". All isoforms showed the ability to activate TEAD as compared to the background of YAP1 −/− control. Nonetheless, we found significant differences in the activity induced by the isoform variants. Both YAP1 isoforms that contained two WW domains induced significantly stronger TEAD activation when compared to the isoforms with only one WW domain (2α vs. 1α and 2γ vs. 1γ). Additionally, we also detected significantly higher activation of transcription by YAP1-2α when compared to 1α (Fig. 5a). These results are in good agreement with previous studies on YAP1 C-terminal deletion mutants, where disruption of the Leucine zipper was shown to have strong effects on transcriptional activity [15].

To further explore the possible effects of differential YAP1-TEAD activation, we focused on the documented function of YAP1 protein in transducing mechanical stimuli arising from the extracellular matrix (ECM) and surrounding cells. Stiff substrates and low cell density are known to induce YAP1 shuttling from the cytoplasm to the nucleus [11,38,40].

We monitored the contribution of single isoforms to cell mechanosensing by checking the effect of their expression on YAP-TEAD transcription activity when cells were challenged by either soft or stiff substrates. Thus, we seeded 8xGTIIC-lux YAP1 −/− CAL51 cells that had been transfected with YAP1 isoforms on soft (0.5 kPa) or stiff (64 kPa) surfaces, which were previously shown to determine a differential activation of YAP1-TEAD transcriptional activity [45]. When we quantified the "readout" of the YAP1-TEAD-based luciferase assay, we noticed that substrate stiffening (64 vs. 0.5 kPa) caused an increased

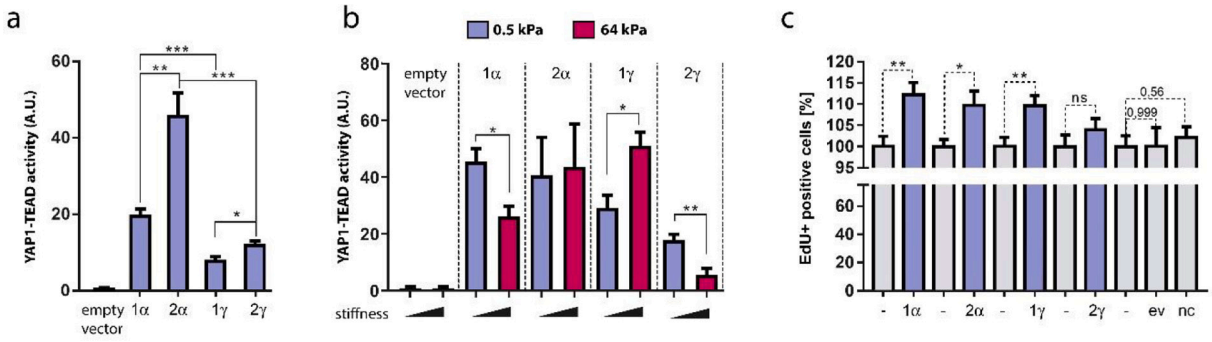

Fig. 5. YAP1 isoforms have unique affinity for TEAD-mediated transcription, mechanosensitivity and proliferation. a) Barplot representation of TEAD transcriptional activity, as measured by Luciferase assay in 8xGTIIC-lux YAP1 −/− CAL51 cells (see [40]) transfected or not with the indicated YAP1 isoforms. Luminescent signal was normalized to YAP1 over-expressing cells with tdTomato reporter and the results were normalized to control (without over-expression). The data are expressed as mean ± SEM. $n = 6$. b) Barplot representation of YAP-TEAD transcriptional activity in 8xGTIIC-lux YAP1 −/− CAL51 cells transfected with the indicated YAP1 isoforms or with the empty vector and cultured for 48 h onto substrates with either 0.5 or 64 kPa Young's Modulus. The data are represented as mean ± SEM). c) Barplot representation of Edu + YAP1 −/− CAL51 cells transfected with the indicated YAP1 isoforms and compared to non-transfected controls. The data are expressed as mean ± SEM. $n = 5$. (* *0,01 < P ≤0,05,* ** 0,001 < P ≤0,01, *** P ≤0,001).

luciferase activity only in cells transfected with 1γ isoform. Cells transfected with 1α and 2γ showed reduced luciferase signal, which remained unaffected in 2α-overexpressing cells on stiff surface (Fig. 5b). This result indicated that the 1γ isoform is the only YAP1 isoform mechanically activated by substrate stiffening in our cell model. Surprisingly, 1α and 2γ are "deactivated" by substrate mechanics and 2α is not responsive.

Numerous TEAD target genes are known to regulate cell proliferation or inhibit apoptosis [74,71]. Therefore, we tested whether the differential ability of the isoforms to promote TEAD transcription would affect cell proliferation. Twenty-four hours after transfecting the isoform expression vectors in YAP1 −/− CAL51 cells, we applied a 4.5 h EdU pulse and quantified the proliferating YAP1 positive cells (tdTomato+ / EdU+), while comparing them to the empty vector or non-transfected cells (TdTomato- / EdU+) by flow cytometry (Fig. 5c). The expression of all isoforms but 2γ determined a similarly significant increase in cell proliferation. As a control, the results obtained by tdTomato empty vector-transfection were indistinguishable from those found in non-transfected cells.

All presented results indicate that YAP1 isoforms display distinct responses to mechanical signals and abilities to promote TEAD-mediated transcription. Although isoforms with 2 WW domains perform better at activating TEAD, this activity does not correlate with the induction of cell proliferation.

2.5. *YAP1 isoforms display a unique transcriptional fingerprint*

Next, we asked whether the specificity shown by YAP1 isoform in promoting TEAD transcription and cell proliferation would be reflected in the activation of isoform-specific genetic programs. Therefore, we complemented H9 embryonic stem cells in which YAP1 had been depleted by the CRISPR/Cas9 gene-editing method (YAP1 KO hES; [51]) by transducing them with 2α, 1α, 2γ, and 1γ isoforms. The list of all significantly regulated genes obtained for each YAP1 isoform is reported in Supplementary Table 1.

We then performed genome-wide RNA sequencing (RNA-seq) on complemented cells and compared the results with YAP1 KO hES transduced with empty vector (EM) and wild type (WT) cells. YAP1 depletion in hES caused significant deregulation of more than 2500 genes ($FC \geq |2|; P \leq 0{,}05$) as compared to the wild-type control (Fig. 6a). As expected, the Principal Component Analysis (PCA) of global gene expression demonstrated that the complementation by every single isoform had an effect on YAP1 KO cells (Fig. 6b). Nevertheless, differences between wild-type and transfected KO cells in given gene clusters could still be visible, suggesting that none of the YAP1 isoforms alone could completely restore the effects of total YAP1 protein depletion (Fig. 6c).

Within the cluster of selected genes whose expression was affected by YAP1 depletion, we selected a few examples that could clarify the transcriptional function of the given isoforms. All isoforms showed the ability to restore the expression of well-known YAP1 targets (CTGF, CYR61 and PAX6), and to repress RHOB and CAT (Fig. 6d). The lower efficiency in complementing these genes by Isoform 1γ was likely due to its relatively lower expression, compared to other isoforms. However, the expression was still higher than that in the wild-type cells, and thus triggering a comparable effect on global gene expression.

Interestingly, no isoforms except for YAP1-1α were able to restore the baseline expression of TEK, a tyrosine kinase receptor involved in YAP regulation of angiogenesis [1,53].

The complementation by the four isoforms affected similar numbers of genes (1α: 2144; 1γ: 2580; 2α: 2922; 2γ: 2328). Among them, 1321 were shared by all the four isoforms tested (Fig. 6e). Interestingly, YAP1-2α recovered six times more unique genes than 1α isoform (626 [141 + 485] vs 102 [72 + 30]). In comparison, the number of unique genes in 1γ vs 2γ isoform was almost the same (335 [250 + 85] vs 302 [224 + 78]) (Fig. 6f). This ratio could suggest that the 2α isoform might exert more specific functions, compared to the others. Interestingly, YAP1 isoforms partially complemented wild-type expression pattern with a more pronounced effect on the group of YAP1 repressed genes (27 to 37%) while the number of genes that are less expressed in YAP1 KO compared to wild-type, was rescued by 10–12% only. These results indicated that a single YAP1 splicing variant might contribute to both common and specific aspects of total protein co-transcriptional functions, but that the expression of multiple isoforms would be needed to better phenocopy the function of YAP1.

Next, we focused on the annotation of genes complemented by single YAP1 isoforms to explore their potentially unique functions. Gene ontology (GO) enrichment analysis [31] of YAP1 −/− cells identified well-known YAP1-linked pathways as ECM organization, cell interactions, collagen formation, etc. Among numerous shared categories (in grey in Fig. 6g) we also identified several ones that were uniquely restored by specific YAP1 isoforms. For example, we recognized that 1α isoform had a unique activity in complementing Rho cycle, PI3K/AKT signaling, FGF2/3/4 signaling, and Gastrin CREB signal transduction pathway, while 1γ isoform complemented transport of small molecules (amino acid and oligopeptide SLC transporters). Instead, isoform 2γ influenced axon-guiding signaling (Ephrin mediated growth-cone collapse) and 2α isoform was unique in restoring the Toll-like receptor cascade regulating the innate immune system. These results suggested the co-existence of YAP1 isoforms in the same cell might be needed to

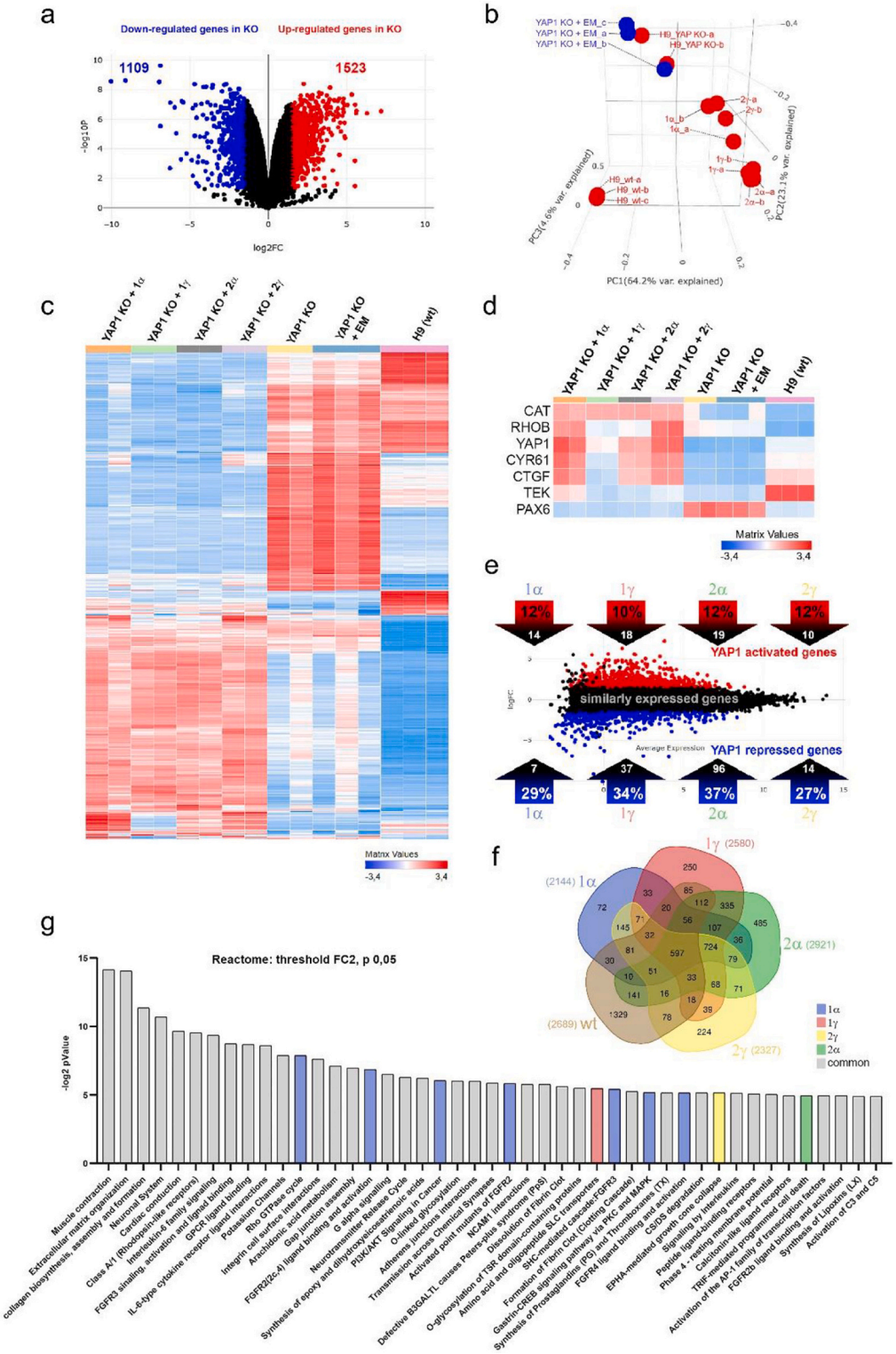

Fig. 6. YAP1 isoforms activate common and unique genetic programs; RNAseq analysis. (a) Volcano plot representation of differentially regulated genes in YAP −/− (YAP-KO) versus CTR hESC cells (WT). Red points indicate significantly up-regulated genes, blue points indicate down-regulated genes. (n = 3, P < 0.05, log2Fc < |1.5|). (b) 3D Principal Component Analysis (PCA) visualizes differences between samples with the highest variability in X axis (64.2%). (c) Heatmap representation of genome-wide analysis in YAP −/− hES transfected with either YAP1-1α, −1γ, −2α, −2γ isoforms or empty vector (EM) as compared to CTR hESC cells (H9 wt). (d) Heatmap representation of the expression of the indicated genes in YAP −/− hES transfected with either YAP1-1α, −1γ, −2α, −2γ isoforms or empty vector (EM) as compared to CTR hESC cells (H9 wt). Heatmaps and PCA graphs were created by BioJupies [64]. (e) MA plot of gene expression ratios displaying the effect of complementation by the indicated YAP1 isoforms as compared to CTR hESC cells. (f) Venn diagram representation of unique and common genes significantly regulated in YAP −/− hES transfected with either YAP1-1α, −1γ, −2α, −2γ isoforms as compared to CTR hESC cells. FC ≥ |2|. (g) Barplot representation of Gene enrichment analysis (REACTOME) showing the most statistically significant terms in YAP −/− hES transfected with either YAP1-1α, −1γ, −2α, −2γ isoforms as compared to CTR hESC cells. Common terms are indicated in grey, Isoform-specific terms (common for at least 2 isoforms) are color-coded. (For interpretation of the references to color in this figure legend, the reader is referred to the web version of this article.)

fine-tune the genetic program activated downstream of total YAP1 protein.

The complete list of all significantly enriched annotations is shown in Supplementary fig. 1. From the filtered, single isoform-specific reactions, we found isoform 1γ to be predominantly involved in several metabolism-regulatory annotations, while 1α-responsive genes almost exclusively targeted signaling by FGF receptors. Isoform 2α regulated NOTCH signaling and generic transcription and 2γ influenced a number of immune system components (eNOS, Nitric oxide, platelet homeostasis, interferon signaling), as well as several reactions of neural system signaling (BH4, Neurofascin, growth cone regulations) (Supplementary fig. 1a). Analysis of the molecular function and biological processes associated to their targets confirmed the specific contribution of each isoform (Supplementary fig. 1b, c).

In the group of common terms representing significant signaling pathways, we could recognize some of the well-known YAP1-linked pathways as extracellular matrix organization [9,40], TGF-beta and SMAD3 signaling [76], apoptosis and cell cycle regulation [25], cell differentiation [34] and Wnt signaling [48]. Consistently, we also detected the regulation of pluripotency and stem cell proliferation [51], Angiotensin II signaling [68], cell-cell adhesion, cadherin signaling pathway.

In order to visualize the most regulated genes, we further increased the fold-change threshold (FC $\geq |16|$) and identified several unique and shared genes supporting the overall robustness of YAP1 signaling (Supplementary fig. 1d).

2.6. *Mass spectrometry analysis reveals YAP1 isoform-specific interacting partners*

Next, we focused on investigating the interactome of YAP1 isoforms that displayed distinct transcriptional activities. The presence of unique interacting proteins could in part explain the function of specific YAP1 splicing variants.

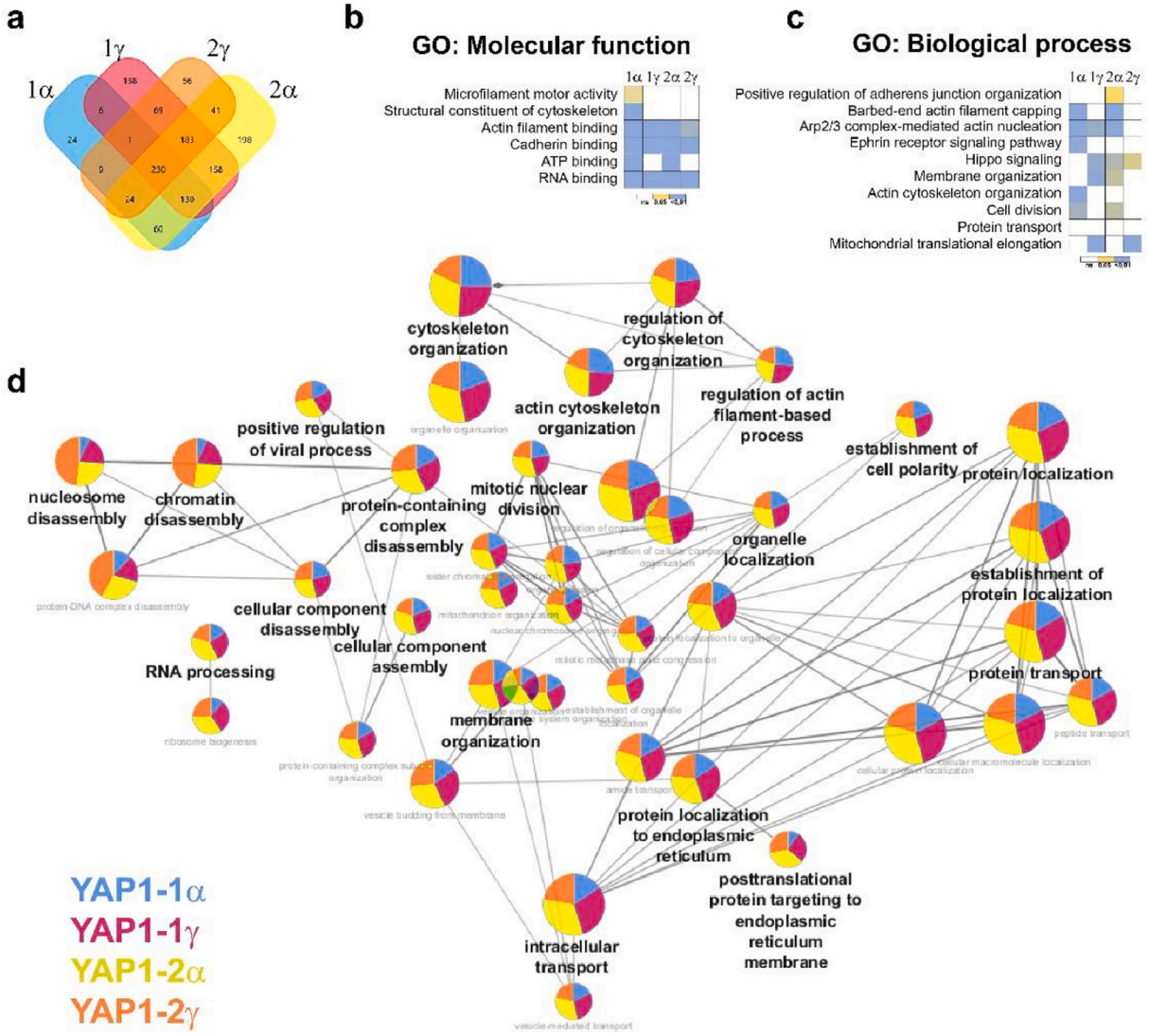

Fig. 7. Enrichment analysis of YAP1 isoform interactors and protein-protein interaction network. (a) Venn diagram representation of isoform-specific interacting proteins, as obtained by tandem mass tag spectrometry (TMT MS), $P < 0,05$, FC2. (b, c) heatmap representation of the Gene Ontology (GO) annotation terms grouped under the Molecular Function and Biological Process categories that are significant for proteins interacting with at least one YAP1 isoform. Isoform-specific YAP1 interactors are identified as those proteins found to be enriched by FC ≥ 2 as compared to YAP1 −/− hES cells transfected with an empty vector. Annotations significant for at least one isoform are aligned to all others. The heat-map intensities are color-coded according to *P*-value adjusted by Bonferroni method. Data were analyzed in MS Excel and FunRich (Functional Enrichment analysis tool). (d) Interaction network visualizing GO: Biological function displays proportional pie-charts that account for the contribution of single YAP1 isoforms. The size of each node reflects the statistical significance of the terms. The interactome maps were created by Cytoscape.

Therefore, we transfected YAP1 −/− hES cells with vectors encoding for 1α, 1γ, 2α, or 2γ isoforms and pulled down the protein with an antibody recognizing a region and the epitopes present in all isoforms. Next, we performed tandem mass tag spectrometry analysis (TMT-MS) of isoform-specific interacting proteins, by using the same cells complemented with empty vector as a control. The list of the isoform-specific interactors identified by TMT-MS is reported in Supplementary Table 2. As a reference, we used Biogrid database of protein-protein interactions that indexes 438 unique interactors of human YAP1. We were able to identify approximately 62 (12,8%) protein interactors for 1α, 92 (10%) for 1γ, 84 (8,2%) for 2α, and 80 (13%) for 2γ isoforms that are already indexed as YAP1 interactors in Biogrid database. This suggests the complementation of YAP1 knock-out by individual over-expressed isoforms was able to recruit numerous known YAP1-binding partners, specific either for one unique or more isoforms (Supplementary Fig. 2).

For subsequent enrichment analysis, we selected YAP1 isoform interactors with log2FC ≥ 1 relative to empty vector, and filtered them for MS contaminants (CRAPome), while preserving proteins indexed in Biogrid. As a result, we found the following numbers of interacting protein with statistical significance (p value ≤0,05): 1α - 484, 1γ - 915, 2α - 1024, 2γ - 613. Out of those, 230 interactors were common to all YAP1 isoforms, while 24, 138, 56, and 198 were unique interactors for 1α, 1γ, 2α and 2α isoform, respectively (Fig. 7a).

In order to better understand the contribution of isoform-specific interactors to YAP1 function, we performed gene annotation (GO) enrichment analyses. We focused on all terms statistically significant at least in one isoform. The analysis of interactor function identified categories such as RNA binding, cadherin binding and actin filament binding, which are known to highlight YAP1 function, to be significant for all isoforms, while others, such as a structural constituent of cytoskeleton and microfilament motor activity were significant only for isoform 1α (Fig. 7b). The analysis of the biological processes demonstrated the proteins interacting with 1α and 2α were characterized by their role in cell division and barbed-end actin filament capping, while 1γ- and 2γ-specific interacting proteins were surprisingly responsible for mitochondrial translational elongation. Proteins interacting with

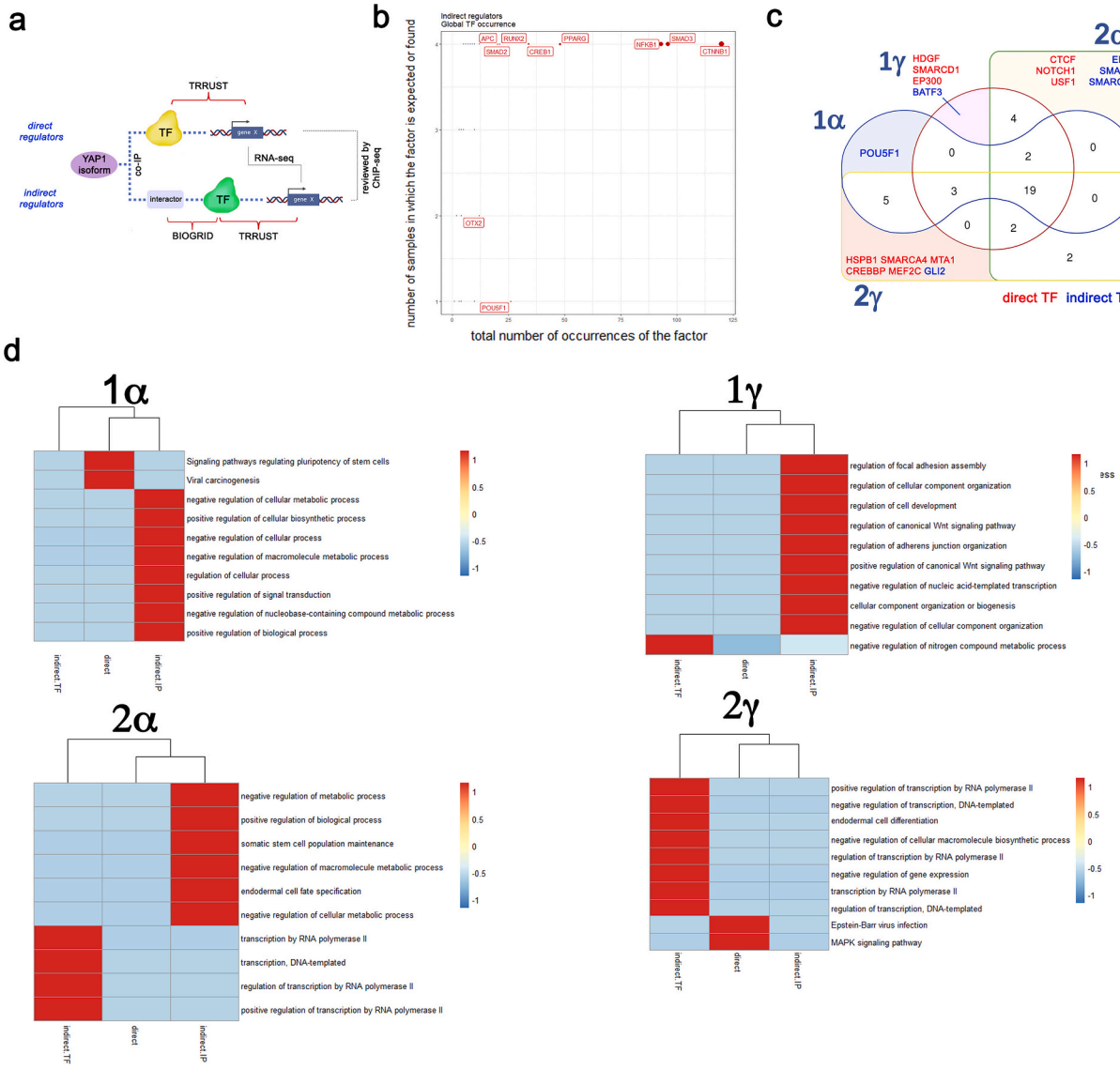

Fig. 8. A multi-omics approach unveils the unique transcriptional activities of YAP1 isoforms. (a) Schematic representation of the multi-omics strategy utilized. (b) Scatter plot representation of hotspot transcription factors (TF) identified as indirect regulators in more than one YAP1 isoform; (c) Venn diagram representation of the unique direct (red) and indirect (blue) transcription factors (TF) identified to interact with the reported YAP1 isoforms by multi-omics; (d) heatmap representation of the 10 most enriched ontologies of direct and indirect transcription factors for each YAP1 isoform as identified by multi-omics analysis through KEGG database. (For interpretation of the references to color in this figure legend, the reader is referred to the web version of this article.)

isoform 2α were uniquely involved in the positive regulation of *adherens junction* organization, while 1α interactors were exclusively deemed responsible for the actin cytoskeleton organization (Fig. 7c). These results indicate that the unique activity of YAP1 isoforms might be due to their ability to interact with different partners (Fig. 7d).

To uncover a set of the most abundant interactors of YAP1 isoforms from the MS dataset, we applied a stronger threshold (log2FC $\geq |2|$). The resulting list of protein interactors revealed the strongest YAP1 interactors by our method. This list can further be used in follow-up studies to highlight specific functions of individual isoforms (Supplementary Fig. 3).

2.7. Multi-omics analysis of YAP1 isoform-specific transcription profiles suggests they exert unique activities

Next, we devised a multi-omics strategy aimed at identifying putative isoform-specific transcriptional activities. The strategy adopted is described in Fig. 8a. Briefly, we compared the YAP1 isoform interactors we had identified by Mass Spectrometry as well as the RNA-seq data against TRUSST database of transcription factors to infer a direct transcriptional regulation due to regulators interacting with YAP1 isoforms. We also assumed indirect regulators as a hidden layer connecting YAP interactors with given genes, and used BIOGRID protein-protein interactions (PPIs) to further match transcription factors to YAP1 interactors and RNA-seq data. We next employed 2 ChIP-seq datasets to confirm the physical binding of the identified regulators to genes of interest. The analysis returned a limited number of proteins acting as direct or indirect regulators of genes in an isoform-specific fashion. As expected most of the identified regulators [19] were common to all 4 isoforms (Fig. 8b and Supplementary Table 3), while 6 specific interactors could be found for isoform 2α (CTCF, NOTCH1, USF1, ERG, SMAD5, SMARCA22) and 2γ (HSPB1, SMARCA4, MTA1, CREBBP, MEF2C, GLI2). Only 4 interacting proteins appeared to be specific for 1γ (HDGF, SMARCD1, EP300, BATF3) and one for 1α (POU5F1, Fig. 8c). The gene ontology enrichment generated testifies the unique transcriptional activity of 4 YAP1 isoforms (Supplementary Table 4).

3. Discussion

Yes-Associated Protein 1 (YAP1) is a transcriptional co-activator acting downstream of the Hippo-tumor suppressor pathway. The pathway regulates cell proliferation, organogenesis, cell stemness [5,21] and its dysregulation has been associated with a number of pathologies, including cancer (reviewed in [26,50]). The main mechanism regulating the function of YAP1 is mediated by Hippo kinases, which negatively control YAP1 activity by phosphorylation of specific Serine residues, followed by sequestration of the protein to the cytoplasm. YAP1 shuttling to the nucleus is prompted by biochemical and mechanical stimuli (Martino et al., 2018 [84]), while it is negatively impacted by cell-cell interaction [73] as well as by cell interaction with soft substrates [11,38]. Hippo phosphorylation activity is sensitive to intracellular tension propagation, thus YAP1 translocation to the nucleus requires cell cytoskeleton integrity [45].

Here, we demonstrate another layer of regulation of YAP1 activity (Fig. 9). The alternative splicing of *YAP1* gene occurs differently in different organs and tissues and it also changes during development and in disease. Our study was prompted by an unbiased bioinformatics analysis of genome-wide transcriptomics datasets, which led us to perform a systematic review of relative expression of the YAP1 isoforms in diverse cell types and during the development.

We demonstrate that the expression of *YAP1* is detectable in most of the tissues and organs, while it is virtually undetectable in the immune cells, including circulating cells and the main hematopoietic organ, the bone marrow. This result could be explained by speculating that the protein is mainly synthesized in parenchymatous tissues, where cells are more exposed to cell-matrix and cell-cell interactions. Indeed, together with its paralog protein TAZ, YAP1 has been described as a mechanosensitive protein, for its ability to promptly respond to modifications in the mechanics of the microenvironment [11,39].

In our study we analyzed YAP1 exon usage in different tissues and organs and found that the transcript most likely undergoes alternative splicing in a tissue-specific fashion. In turn, our analysis of human genome databases confirmed the existence of 12 YAP1 isoforms, among which only 9 produce mRNAs. This evidence led us to ask if different isoforms of YAP1 exert distinct functions and whether the balanced

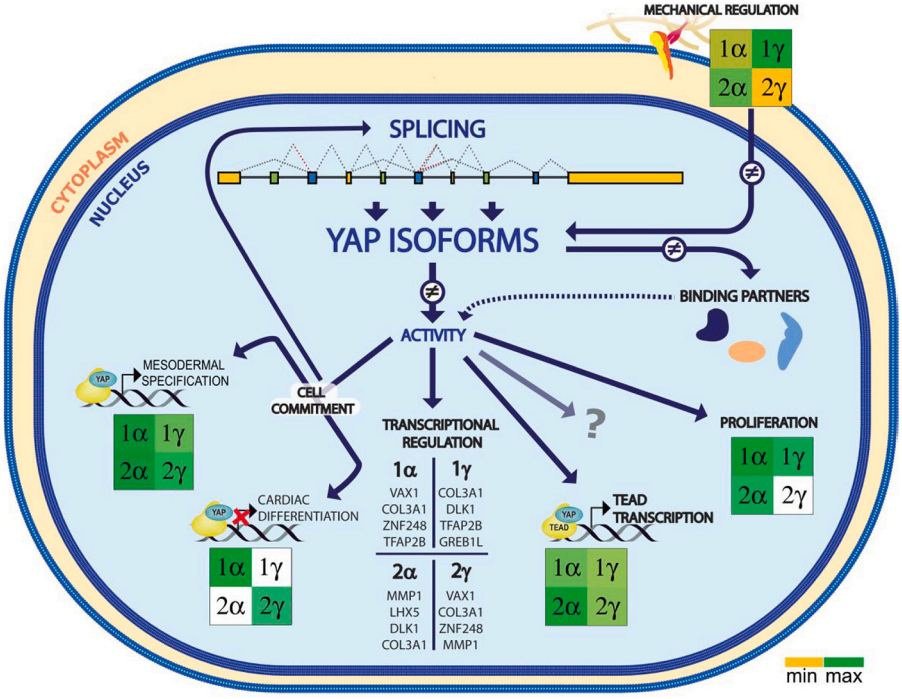

Fig. 9. *Schematic model of YAP1 isoforms signaling.* *YAP1* undergoes alternative splicing resulting in coding isoforms that can interact with either diverse or the same binding partners, albeit with variable affinity. The downstream signaling results in the regulation of target genes (top four genes for each complementation experiment are shown; data are based on RNAseq experiments). The mechanical regulation and the contribution of the four most represented YAP1 isoforms to the regulation of cell commitment, TEAD transcription, and proliferation are indicated by color-coding. The question mark indicates the possibility that other activities for YAP1 splicing isoforms exist.

expression of different YAP1 isoforms in distinct cell types and tissues would correspond to their physiological functions.

Therefore, we first selected human cell types of different embryological origin and analyzed the levels of *YAP1* gene expression. Among various cells, the YAP1 gene was relatively highly expressed in cardiac fibroblasts and breast cancer line CAL51, while lower levels could be detected in the embryonic kidney line HEK293, and human skin carcinoma line A2058. When we quantified the relative expression of YAP1 splicing isoforms in these cell types, we found the predominance of isoform 2α in all the cell types and significant differences in the relative expression of the other isoforms.

We also found differences in YAP1 isoform relative expression in human embryonic and induced pluripotent stem cells (hES and iPS, respectively), which are known to represent different stages of cell pluripotency. Additionally, this phenomenon could be witnessed during the maturation of iPS to the muscle and neuronal phenotypes. Both these processes have been associated with the inactivation of YAP1 transcriptional function [8,13,27,39,80].

By examining closer the expression of YAP1 isoforms during cardiac differentiation, we described the dynamics of the splicing of YAP1 transcripts and clarified that YAP1 isoforms 1α and 2γ act more efficiently in repressing iPS differentiation to cardiomyocytes than variants 1γ and 2α, the latter two being the most regulated isoforms during cardiac differentiation. On the other hand, by quantifying the relative expression of YAP1 splicing variants in human heart, we found a specific signature for the pathological tissue, which most likely reflects the altered balance between contractile cells and cardiac fibroblasts in the diseased heart. Along with the recent report for the laboratory of Hatakeyama and colleagues on different functions of YAP1 isoforms in cancer signaling [3], we also suggest that YAP1 isoforms might play discrete roles in another pathology, namely heart failure. Interestingly, a role for YAP1 protein in the progression of the heart pathology was recently reported by our group [82].

YAP1 function has been historically associated with the presence of WW domain(s) [54] and the ability of the protein to physically interact with transcription factors belonging to the TEAD family ([67]; Zanconato et al., 2015). YAP-TEAD transcriptional activity can be monitored by quantifying TEAD reporter and has been shown to be compelling in YAP1 response to mechanical cues and in mediating cell proliferation [11]. Our results obtained by complementing YAP1 knock-out cell lines with single splicing variants confirmed and expanded previous observations that YAP1 isoforms with 2 WW domains are more efficient in activating TEAD transcription than those with 1 WW domain [30]. Nonetheless, neither the interaction of YAP1 with TEAD nor the number of its WW domains can predict the ability of the isoforms to induce cell proliferation or mediate mechanosensitivity. Unfortunately, our experimental design cannot exclude that certain non-physiological effects could be induced by the dosage of the transfected isoforms.

Nevertheless, in our experimental model, only one of 9 variants of YAP1, namely YAP1-1γ (that contains a single WW domain and a disrupted Leucine-zipper region that prevents the formation of heterodimers with TAZ protein) appears to be able to prompt TEAD-mediated transcription in response to substrate stiffening. In addition, our data show that the YAP1-1γ isoform may have a unique role in mitochondrial elongation. Together, these observations shed a new light on how mechano-signaling and mitochondrial dynamics might act in concert to control heart regeneration.

Since all isoforms tested share the same TID region, these data indicate the function of YAP1 isoform could be shaped by their interaction with specific protein co-factors. Accordingly, we show that YAP1 splicing isoforms interact with different subsets of protein partners, and activate both common and unique genetic programs. As a result, single splicing variants fail to complement all the functional and molecular activities in which total YAP1 protein is engaged. In order to corroborate these data, we adopted a multi-omics strategy by which we identified novel transcription factors that appear to be indirect regulators of YAP1 transcriptional activity. This approach has taken us a step closer to unveiling the complexity of individual YAP1 isoforms as transcriptional co-activators.

In conclusion, we report on a new layer of complexity to the signaling by the YAP1 proto-oncogene protein via its numerous mRNA splice isoforms in normal as well as diseased tissues and organs, including the pathology of the heart.

4. Materials and methods

4.1. YAP1 expression vectors

Coding sequences (CDS) of all nine YAP1 variants (1α, 2α, 1β, 2β, 1γ, 2γ, 1δ, 2δ, ι4) were cloned under the control of the CAG promoter. The reading frame was N-terminally-linked by E2A sequence with tdTomato fluorescent reporter. This cassette was cloned into the pUC19 backbone. Constructs were verified by restriction digestion analysis followed by fragment separation on 1% agarose gel. Finally, coding sequences were sequenced. The expression of the transgene was confirmed by Real-Time PCR (RT-qPCR) and the presence of YAP1 protein was assessed by western-blot analysis using 10% polyacrylamide gels (Bio-Rad) followed by transfer to a polyvinylidene difluoride (PVDF) membrane using the Trans-Blot Turbo transfer system (Bio-Rad). Membranes were blocked with 5% BSA in TBST, incubated with diluted primary YAP1 antibody (Cell signaling #14074, 1:1000) in 5% BSA in TBST at 4 °C overnight. After 1 h of incubation at room temperature with HRP-linked antibody (7074; Cell Signaling Technology) the membranes were developed using Clarity™ Western ECL Substrate (BioRad) and imaged in a ChemiDoc imaging system (BioRad).

4.2. Cell culture and differentiation

The human iPS cell line DF 19–9-7 T (iPS, karyotype: 46, XY) was purchased from WiCell (Madison, WI, USA). The YAP knock out (YAP−/− or KO) and isogenic H9 (WT or CTR) human embryonic stem cell lines (hES) were a kind gift of Miguel Ramalho-Santos and Han Qin. Their generation and culture were described in [51]. Troponin I1 reporter iPS line (TNNI-iPS) was purchased from Coriell Institute (cat.nr. AICS-0037-172, Camden, New Jersey, USA). The cells were maintained in an undifferentiated state by culturing them onto Matrigel Growth Factor Reduced (1:100 in DMEM/F12, Corning) in complete Essential 8™ Medium (E8, ThermoFisher Scientific) containing penicillin/streptomycin (0.5%, VWR). Cardiac differentiation was performed according to the protocol of Lian et al., 2012 [6]. Neural differentiation for relative expression of YAP1-TVs was performed as follows. NSCs were differentiated into neurons based on modified previously published protocol [72]. In brief, confluent NSCs were induced using neural progenitor media (NPM) consisting in DMEM/F12, 0,5% B27 50× (Gibco), 0.5% N2 Supplement 100× (Gibco), 2 mM GlutaMAX-I Supplement (Gibco) and 1% pen/strep (VWR)) for 5–7 days changing half of the medium volume every day. Prior the final differentiation stage, polyornithine-laminin coated 24-multiwell plates (24-MW) were prepared as follows. The plates with poly-L-ornitine solution (0.1 mg/ml in PBS, Sigma) were incubated overnight at 37 °C. The next day, 24-MW plates were washed twice with dH2O and incubated with laminin solution (10mg/ml in PBS, Invitrogen) for 3 h at 37 °C. Afterward, cells were washed with PBS, incubated for 2–3 min at 37 °C with Accutase (Gibco), then pelleted (250xg, 5 min), counted and resuspended in neuronal differentiation media (NDM), which consisted of Neurobasal medium (Gibco), 1% B27 50× (Gibco), 1% N2 Supplement 100× (Gibco), 1% pen/strep (VWR), 10 ng/ml BDNF (Gibco), 10 ng/ml GDNF (Gibco), 10 ng/ml IGF-1 (Gibco), 1μg/ml XX (Invitrogen), 1uM cAMP (Sigma) and 200 ng/ml of L-Ascorbic acid (Sigma)). Cells were then seeded at the density of $10x10^4$ cells per well and maintained in culture for 21–25 days for final neuronal differentiation , changing media once or twice a week.

Primary Human Cardiac Fibroblasts (CFs) were either isolated from

the ventricles of the adult heart or purchased from Sigma-Aldrich (C-12375). Patient-derived primary cardiac fibroblasts were obtained by explant outgrowth on a pre-gelatinized plate and sorted on a MoFlo Astros EQ (Beckman Coulter) for Thy1 (CD90)-positive and PECAM-1 (CD31)-negative endothelial cells. Freshly isolated cells were cultured in Claycomb media (Sigma 51800C) supplemented with 15% FBS (Sigma), L- Glutamine (2 mM, Biowest) and 1% Penicillin/Streptomycin. After isolation, the cells were maintained in DMEM/F12 supplemented with 10% FBS (Sigma), L-Glutamine (2 mM, Biowest) and 1% Penicillin/Streptomycin. Once the cells reached 80% confluence, the CFs were expanded 1:3–1:5 or at a seeding density of $5x10^3$ cells/cm^2 and the cell culture medium was replaced daily.

Breast cancer cell line CAL51 and YAP−/− (KO) CAL51 cell lines were cultured as previously described [40].

4.3. Tissue-specific distribution of YAP1

The graph of Tissue-specific expression of YAP1 was created by combining the data from three transcriptomics datasets (HPA, GTEx, and FANTOM5) available from v19.1 www.proteinatlas.org. For comparison of YAP1 exon usage we used the Genotype-Tissue Expression project: (GTEx) www.gtexportal.org/home/gene/YAP1#eQTLBlock, data source: GTEx Analysis Release V8; dbGaP Accession phs000424.v8.p2).

4.4. Cell transfection

Transfection of all cell lines used in this work was performed with FuGENE® HD Transfection Reagent (Promega Cat. No 2312) by following the manufacturer's instructions. To increase the transfection efficiency, the cells were passaged 24 h prior transfection and/or 1 min pre-treatment of the cells by TrypLE Express (Thermofisher) was applied without cell detaching.

4.5. Luciferase assay

YAP1 transfected CAL51 cells were cultured in DMEM containing 4.5 g/l Glucose (DMEM high Glucose, Lonza) supplemented with 10% fetal bovine serum (Sigma-Aldrich), L-glutamine (2 mM) and penicillin/streptomycin (100 U/ml). After reaching 50% confluency, the cells were transfected with an 8xGTIIC-lux plasmid (Addgene #34615, a kind gift from Stefano Piccolo) in which a YAP/TEAD-responsive synthetic promoter drives luciferase expression and the pRL-TK Renilla (Promega) control at a 1:1 ratio (200 ng/well). Before the analysis, transfected cells were seeded either in 96 well or on soft (0.5 kPa) or stiff (64 kPa) surfaces. CytoSoft® 6-well plates with a thin layer of anhydride-functionalized silicone with different stiffness were purchased from Advanced BioMatrix and used according to the manufacturer's instructions. Luciferase assay was performed 24 h after treatments using the Dual-Glo® Luciferase Assay System kit (Promega) according to the manufacturer's protocol and analyzed on a Berthold CENTRO LB 960 Microplate Luminometer (Berthold Technologies GmbH).

4.6. RNA extraction and quantitative real-time PCR (RT-qPCR)

Total RNA was extracted using a High Pure RNA Isolation Kit (Roche) according to the manufacturer's instructions. Reverse transcription (1 μg of RNA) was performed using Transcription First Strand cDNA Synthesis Kit (Roche) and RT-qPCRRT was carried out in triplicate, using a LightCycler 480 SYBR Green I Master Kit (Roche) and run on a LightCycler 480 Real-Time PCR System (Roche). The cDNA of human metastatic melanoma line (A2058) was purchased from Sigma-Aldrich (cat. No. 91100402-1VL). The cDNA from skeletal muscle was isolated from d16 iPS-derived skeletal muscle cells (skMC) differentiated from IPS as described in Chan et al., Nat Protocols 2016 [28]. The total RNA from the human heart was a pool from multiple hearts (Clontech, No. NC9900441).

The expression level of individual genes was determined by ΔCt method relative to the expression of the housekeeping gene GAPDH and 18S. Following primers (*de-novo* designed or modified from Karystinou 2015 [32] were used to specifically amplify YAP1 isoforms: YAP1-F1: CCTCTTCCTGATGGATGGGA, YAP1-F2: GATGAACTCGGCTTCAGCCATGAA, YAP1-F3: AGCCCACTCGGGATGTAACTTGA, YAP1-R1: TATTCCGCATTGCCTGCCGAAGCA, YAP1-R2: GCAGGGCTAACTCCTGCCGAAGCA, YAP1-R3: CTGGTGGGGGCTGTGACGTT, YAP1-R4: GCAGGGCTAACTCCTGTGGCCTCA, YAP1-R5: ATTGCCTGTGGCCTCACCT). Isoform-specific combinations of primers were as follows: 1α: F2-R2, 2α: F1-R2, 1β: F2-R4, 2β: F1-R4, 1γ: F2-R1, 2γ: F1-R1, 1δ: F2-R5, 2δ: F1-R5, i4: F3-R3. Primers for transcript isoform 2γ also co-detect isoform i4, but not vice-versa.

4.7. RNA-Seq

YAP1 CRISPR mutant line H9 was complemented with individual YAP1-1α, YAP1-1γ, YAP1-2α, YAP1-2γ isoforms as described above. Two biological replicas for each complementation assay and three replicas for empty vector control and wild-type H9 line were used for RNA-seq analysis. The sequencing library was wasprepared by using NEBNext Ultra II Directional Kit (New England Biolabs, MA, USA). In brief, 200–300 ng total RNA was used as an input into the polyA enrichment module protocol. The enriched sample was then fragmented and transcribed into cDNA. Following universal adapter ligation, samples were barcoded using dual indexing primers. Samples were sequenced to 25–35 million single-end 75 bp reads on Illumina Nextseq 550 sequencer (Illumina, CA, USA). The data analysis was performed using Biojupies [64]. Enrichment analyses were performed using the gene-set enrichment tool ShinyGO (ShinyGO v0.61; http://bioinformatics.sdstate.edu/go/, doi:https://doi.org/10.1093/bioinformatics/btz931) and heatmaps were generated by MS excel.

4.8. Mass spectrometry

4.8.1. Tryptic digestion and Tandem Mass Tag (TMT) labeling

The samples were digested with trypsin using S-TRAP microcolumns (Protifi) according to the manufacturer's protocol. Briefly, the samples were reduced with dithiothreitol (DTT) and alkylated with methyl methanethiosulfonate (MMTS). After alkylation, the samples were acidified with phosphoric acid and mixed with S-TRAP binding buffer (90% methanol, 10% 1 M triethylammonium bicarbonate (TEAB)). The samples were loaded onto S-TRAP microcolumns, washed four times with S-TRAP binding buffer, and digested with trypsin overnight. Peptides were eluted from the columns in three steps with 50 mM TEAB, 0.2% formic acid (FA), and 50% acetonitrile (ACN), 0.2% FA. The eluted peptides were dried down and resuspended in 50 mM TEAB. Peptides were labeled with TMTpro 16plex label reagent (Thermo Fisher Scientific) according to the manufacturer instructions. Samples were pooled to a TMT-set and fractionated by basic reversed-phase chromatography (bRP-LC) using a Dionex Ultimate 3000 UPLC system (Thermo Fisher Scientific). Peptide separation was performed using a reversed-phase XBridge BEH C18 column (3.5 μm, 3.0 × 150 mm, Waters Corporation) and a linear gradient from 3% to 40% solvent B. Solvent A was 10 mM ammonium formate buffer (pH 10.0) and solvent B was 90% ACN, 10% solvent A. The sample was fractionated into 20 primary fractions and concatenated into the final 10 fractions. The fractions were dried and reconstituted in 3% ACN, 0.2% FA for LC-MS analysis.

4.8.2. LC-MS/MS Analysis

The fractions were analyzed on an Orbitrap Fusion Lumos Tribrid mass spectrometer interfaced with Easy-nLC1200 liquid chromatography system (both Thermo Fisher Scientific). Peptides were trapped on an Acclaim Pepmap 100 C18 trap column (100 μm × 2 cm, particle size 5 μm, Thermo Fisher Scientific) and separated on an in-house packed analytical column (75 μm × 30 cm, particle size 3 μm, Reprosil-Pur C18,

Dr. Maisch) using a linear gradient from 5% to 33% B over 77 min followed by an increase to 100% B for 3 min, and 100% B for 10 min at a flow of 300 nL/min. Solvent A was 0.2% FA in water and solvent B was 80% ACN, 0.2% FA. MS scans were performed at a resolution of 120,000, *m/z* range 375–1375. MS/MS analysis was performed data-dependent, with a top speed cycle of 3 s of the most intense precursors with a charge state of 2–7. Precursors were fragmented in MS2 by collision-induced dissociation (CID) at a collision energy of 35. The maximum injection time was set to 50 ms and fragment ions were detected in the ion trap followed by multi-notch (simultaneous) isolation of the top 10 MS2 fragment ions, with m/z 400–1400, selected for fragmentation (MS3) by higher-energy collision dissociation (HCD) at 65% and detection in the Orbitrap. MS3 resolution was set to 50,000 and m/z range of 100–500. Precursors were isolated in the quadrupole with an isolation window of 0.7 m/z and a dynamic exclusion within 10 ppm during 45 s was used for m/z-values already selected for fragmentation.

4.9. Proteomic Data Analysis

The raw-data files of the TMT fractions were merged for identification and relative quantification using Proteome Discoverer version 2.4 (Thermo Fisher Scientific). The search was performed by matching against the *Homo sapiens* Swissprot Database (version 3/2019, Swiss Institute of Bioinformatics, Switzerland) including sequences of YAP1 isoform with N-terminally linked tdTomato using Mascot 2.5 (Matrix Science) with a precursor mass tolerance of 5 ppm and fragment mass tolerance of 0.6 Da. Tryptic peptides were accepted with zero missed cleavage. TMTpro-label modifications of peptide N-terminus and lysine were selected. TMT reporter ions were identified in the MS3 HCD spectra with 3 mmu mass tolerance, and the TMT reporter intensity values for each sample were normalized on the total peptide amount. Only peptides unique for a given protein were considered for quantification.

MS data filtering: in order to decrease potential unspecific contaminants, proteins that were 1× more enriched over the control were filtered by using the CRAPome database (v 1.1; http://www.crapome.org/) with threshold ≤50. Proteins with values >50 were compared to Biogrid database (v3.5.186; https://thebiogrid.org/115684) of known YAP1 interactors and overlapping proteins were included into the analyses by FUNRICH *(Functional Enrichment analysis tool; v3.1.3, funrich.org), using Uniprot Human; Taxon ID:9606, Release 2019_10 of 13-Nov-2019. The interactome maps was created by Cytoscape v3.72 with ClueGO v2.5.6 with the following setting: P < 0,01, Kappa score 0,4, GO Tree Interval 2–6, Bonferroni p-value correction, GO Term Grouping 3/50/50.*

4.10. Patient-derived heart tissue collection

Human healthy controls and diseased heart tissue samples were obtained from the apex of cadaveric donors of non-transplantable hearts and from heart failure patients eligible for organ transplantation. All experiments were performed in accordance with the ethical standards of the Centre of Cardiovascular and Transplantation Surgery and approved by the Ethics Committee of St. Anne's University Hospital, Brno, Czech Republic.

4.11. Histology and Masson's trichrome staining

Heart tissues were dissected in cold DPBS, fixed for 4–8 h in 4% PFA at 4 °C, cryoprotected in 30% sucrose overnight at 4 °C, embedded in Tissue Freezing Medium (Leica Biosystems) and snap-frozen in isopentane over dry ice. Frozen tissue was then cut into 5 μm-thick sections using a cryostat (Leica Biosystems).

Masson's Trichrome staining was performed according to the manufacturer's instructions (Sigma-Aldrich) using celestine blue (0.5% m/v celestine blue, 5% m/v ammonium iron-III sulfate dodecahydrate and glycerol in distilled water, Sigma-Aldrich) and Bouin's solution (VWR Chemicals). Whole tissue was visualized under a slide scanner Zeiss Axio Scan Z1 microscope using the bright-field mode and a 10× objective.

4.12. Confocal imaging

TNNI-GFP iPS-derived cardiomyocytes, transfected with YAP1 expression vectors, were visualized under a Zeiss LSM 780 confocal microscope after 16 days of cardiac differentiation.

4.13. FACS analysis

TNNI-GFP cells and tdTomato positive YAP1 transfected cells were analyzed using flow cytometry as follows. Single cardiomyocyte differentiating cells were prepared by using Multi-tissue dissociation kit 3 (Miltenyi Biotec Ca No. 130–110-204) at day 16 of cardiac differentiation and mCherry positive and GFP and tdTomato positive cells were analyzed by Beckman Coulter MoFlow Astrios Cell Sorter (Beckman Coulter Life Sciences). The percentage of positive cells was quantified by using FlowJo software V10 (Tree Star).

4.14. Transcriptional regulation inference and gene ontology enrichment

All analyses were performed in R. Transcription factor (TF) – TF target pairs were downloaded from the TRRUST database V2, mouse dataset (https://www.grnpedia.org/trrust/) [78]. Protein-protein interaction (PPI) data were downloaded from BIOGRID (https://thebiogrid.org/), release BIOGRID-4.2.193, mouse dataset [79]. Two approaches were set to infer transcriptional regulation from the proteins interacting with YAP to the genes upregulated (log2 fold-change threshold >1) in RNA-seq analysis. For direct transcriptional regulation, we searched for TF pairs in TRRUST using upregulated genes and then subset to TF present among YAP interactors. For indirect transcriptional regulation, we supposed a hidden layer (1 more interactor) connecting YAP interactors with TF. To this aim, after identifying the TF as before, we fetched all the PPI of the TF from BIOGRID and then pruned the results to those having also PPI with YAP interactors. To ensure robustness, both the TF and the intermediate (hidden) interactor were checked for presence in YAP ChIP-seq datasets [40,80] and the results subset to those appearing at least once in ChIPseq data. Gene ontology (GO) enrichment was performed using the *STRINGdb* package to interrogate the STRING database [81] restricting to Kyoto Encyclopedia of Genes and Genomes (KEGG) pathways with fdr-corrected *p*-value <0.01. Enrichments were performed for the combined set of YAP interactors and upregulated genes and, for transcriptional regulation, for TF and inferred regulators, and enrichments are reported as -log10 fdr.

Supplementary data to this article can be found online at https://doi.org/10.1016/j.ygeno.2021.03.009.

Author contributions

JV: experiment conceptualization and execution, manuscript drafting; **VV**: experiment conceptualization and execution; **ARP**: data analysis and interpretation; **JODC**: reporter line generation and analysis, manuscript drafting; **FM**: sample preparation, RNA-sequencing and Mass Spectrometry analysis; **AP, VI**: bioinformatics analysis and data representation; **OH**: clinical consultation; **VR**: embryonic stem cell culture and differentiation manuscript revision; **MS**: conceptualization, manuscript drafting and revision; **SP**: induced pluripotent stem cell culture, differentiation and analysis; **GF**: conceptualization, manuscript drafting and revision.

Acknowledgements

Quantitative proteomics analysis was performed at the Proteomics Core Facility of Sahlgrenska Academy, University of Gothenburg. The Proteomics Core Facility is grateful to the Inga-Britt and Arne Lundbergs

Forskningsstiftlese for the donation of the Orbitrap Fusion Tribrid MS instrument. This work was supported by the European Regional Development Fund - Project MAGNET (No. CZ.02.1.01/0.0/0.0/15_003/0000492) and the European Regional Development Fund in frame of the project Kompetenzzentrum MechanoBiologie (ATCZ133) in the Interreg V-A Austria - Czech Republic programme. M.S. would like to acknowledge generous grants from the National University of Singapore (R-185-000-2710-133 and -733), the Mechanobiology Institute (MBI) (R-714-018-006-271), and the Institute of Molecular and Cell Biology (M-R02010). Additionally, the authors would like to thank Nives Škorja for providing skMC cDNA.

References

[1] T. Azad, M. Ghahremani, X. Yang, The role of YAP and TAZ in angiogenesis and vascular mimicry, Cells 8 (5) (2019) 407. Published 2019 May 1, https://doi.org/10.3390/cells8050407.

[2] S. Basu, N.F. Totty, M.S. Irwin, M. Sudol, J. Downward, Akt phosphorylates the Yes-associated protein, YAP, to induce interaction with 14-3-3 and attenuation of p73-mediated apoptosis, Mol. Cell 11 (1) (2003 Jan) 11–23, https://doi.org/10.1016/s1097-2765(02)00776-1 (12535517).

[3] C. Ben, et al., Alternative splicing reverses the cell-intrinsic and cell-extrinsic prooncogenic potentials of YAP1, J Biol. Chem. 295 (41) (2020 Oct 9) 13965–13980, https://doi.org/10.1074/jbc.RA120.013820. Epub 2020 Aug 6.

[4] P. Bork, M. Sudol, The WW domain: a signalling site in dystrophin? Trends Biochem. Sci. 19 (12) (1994 Dec) 531–533, https://doi.org/10.1016/0968-0004(94)90053-1 (7846762).

[5] F. Camargo, et al., YAP1 increases organ size and expands undifferentiated progenitor cells, Curr. Biol. 17 (2007) 2054–2060.

[6] X. Lian, C. Hsiao, G. Wilson, K. Zhu, L.B. Hazeltine, S.M. Azarin, K.K. Raval, J. Zhang, T.J. Kamp, P. Palecek, Robust cardiomyocyte differentiation from human pluripotent stem cells via temporal modulation of canonical Wnt signaling, Proc Natl Acad Sci U S A 109 (27) (2012 Jul 3) E1848–E1857, https://doi.org/10.1073/pnas.1200250109. Epub 2012 May 29.

[7] Choong-Kun, et al., Tumor metastasis to lymph nodes requires YAP-dependent metabolic adaptation, Science 363 (6427) (2019 Feb 8) 644–649, https://doi.org/10.1126/science.aav0173. Epub 2019 Feb 7.

[8] D.P. Del Re, Y. Yang, N. Nakano, J. Cho, P. Zhai, T. Yamamoto, N. Zhang, N. Yabuta, H. Nojima, D. Pan, J. Sadoshima, Yes-associated protein isoform 1 (Yap1) promotes cardiomyocyte survival and growth to protect against myocardial ischemic injury, J. Biol. Chem. 288 (6) (2013 Feb 8) 3977–3988, https://doi.org/10.1074/jbc.M112.436311. Epub 2012 Dec 30. PMID: 23275380; PMCID: PMC3567650.

[9] O. Dobrokhotov, M. Samsonov, M. Sokabe, H. Hirata, Mechanoregulation and pathology of YAP/TAZ *via* Hippo and non-Hippo mechanisms, Clin Transl Med. 7 (1) (2018) 23. Published 2018 Aug 13, https://doi.org/10.1186/s40169-018-0202-9.

[10] J. Dong, et al., Elucidation of a universal size control mechanism in Drosophila and mammals, Cell 130 (2007) 1120–1139.

[11] S. Dupont, et al., Luciferase reporter assays to determine YAP/TAZ activity in mammalian cells: methods and protocols, Method. Mol. Biol. (Clifton, N.J.) (2019) 121–135, https://doi.org/10.1007/978-1-4939-8910-2_11.

[12] R. Ehsanian, et al., YAP dysregulation by phosphorylation or ΔNp63-mediated gene repression promotes proliferation, survival and migration in head and neck cancer subsets, Oncogene (2010), https://doi.org/10.1038/onc.2010.339.

[13] C. Estarás, H.T. Hsu, L. Huang, K.A. Jones, YAP repression of the WNT3 gene controls hESC differentiation along the cardiac mesoderm lineage, Genes Dev. 31 (22) (2017 Nov 15) 2250–2263, https://doi.org/10.1101/gad.307512.117. Epub 2017 Dec 21. PMID: 29269485; PMCID: PMC5769769.

[14] M.L. Finch-Edmondson, et al., TAZ protein accumulation is negatively regulated by YAP abundance in mammalian cells, J Biol Chem (2015), https://doi.org/10.1074/jbc.M115.692285.

[15] Finch-Edmondson, et al., Biochemistry and Biophysics Reports. Splice variant insertions in the C-terminus impairs YAP's transactivation domain, 2016 (Reference is incomplete).

[16] K. Fujita, Y. Mao, S. Uchida, X. Chen, H. Shiwaku, T. Tamura, H. Ito, K. Watase, H. Homma, K. Tagawa, M. Sudol, H. Okazawa, Developmental YAPdeltaC determines adult pathology in a model of spinocerebellar ataxia type 1, Nat. Commun. 8 (1) (2017 Nov 30) 1864, https://doi.org/10.1038/s41467-017-01790-z. PMID: 29192206; PMCID: PMC5709507.

[17] Gaffney, et al., Identification, basic characterization and evolutionary analysis of differentially spliced mRNA isoforms of human YAP1 gene, GENE (2012), https://doi.org/10.1016/j.gene.2012.08.025.

[18] G. Halder, S. Dupont, S. Piccolo, Transduction of mechanical and cytoskeletal cues by YAP and TAZ, Nat. Rev. Mol. Cell Biol. 13 (9) (2012 Sep) 591–600, https://doi.org/10.1038/nrm3416. Epub 2012 Aug 16. (22895435).

[19] T. Halevy, A. Urbach, Comparing ESC and IPS-based models for human genetic disorders, J. Clin. Med. 3 (4) (2014 Oct 24) 1146–1162, https://doi.org/10.3390/jcm3041146. PMID: 26237596; PMCID: PMC4470175.

[20] Y. Hao, A. Chun, K. Cheung, B. Rashidi, X. Yang, Tumor suppressor LATS1 is a negative regulator of oncogene YAP, J. Biol. Chem. 283 (2008) 5496–5509.

[21] T. Heallen, et al., Hippo pathway inhibits wnt signaling to restrain cardiomyocyte proliferation and heart size, Science (2011), https://doi.org/10.1126/science.1199010.

[22] N. Hou, Y. Wen, X. Yuan, H. Xu, X. Wang, F. Li, et al., Activation of Yap1/Taz signaling in ischemic heart disease and dilated cardiomyopathy, Exp. Mol. Pathol. 103 (2017) 267–275, https://doi.org/10.1016/j.yexmp.2017.11.006.

[23] M. Hoshino, M.L. Qi, N. Yoshimura, T. Miyashita, K. Tagawa, Y. Wada, Y. Enokido, S. Marubuchi, P. Harjes, N. Arai, K. Oyanagi, G. Blandino, M. Sudol, T. Rich, I. Kanazawa, E.E. Wanker, M. Saitoe, H. Okazawa, Transcriptional repression induces a slowly progressive atypical neuronal death associated with changes of YAP isoforms and p73, J. Cell Biol. 172 (4) (2006 Feb 13) 589–604, https://doi.org/10.1083/jcb.200509132. Epub 2006 Feb 6. PMID: 16461361; PMCID: PMC2063678.

[24] M. Iglesias-Bexiga, F. Castillo, E.S. Cobos, T. Oka, M. Sudol, I. Luque, WW domains of the yes-kinase-associated-protein (YAP) transcriptional regulator behave as independent units with different binding preferences for PPxY motif-containing ligands, PLoS One 10 (1) (2015), https://doi.org/10.1371/journal.pone.0113828 e0113828.

[25] Linglu Jia, et al., Activated yes-associated protein accelerates cell cycle, inhibits apoptosis, and delays senescence in human periodontal ligament stem cells, Int. J. Med. Sci. 15 (11) (30 Jul. 2018) 1241–1250, https://doi.org/10.7150/ijms.25115.

[26] J. Jin, X. Zhao, H. Fu, Y. Gao, The effects of YAP and its related mechanisms in central nervous system diseases, Front. Neurosci. 14 (2020) 595, https://doi.org/10.3389/fnins.2020.00595.

[27] P.H. Kang, David V. Schaffer, Sanjay Kumar, Angiomotin links ROCK and YAP signaling in mechanosensitive differentiation of neural stem cells, Mol. Biol. Cell 31 (5) (2020) 386–396.

[28] X. Chal, C. Tanoury, G. Hestin, K. Gober, L.B. Aivio, S.M. Hick, K.K. Cherrier, J. Nesmith, T.J. Parker, P. Pourquié, Generation of human muscle fibers and satellite-like cells from human pluripotent stem cells in vitro, Nat Protoc. 11 (10) (2016) 1833–1850, https://doi.org/10.1038/nprot.2016.110. Oct, Epub 2016 Sep 1.

[29] M. Kofler, P. Speight, D. Little, et al., Mediated nuclear import and export of TAZ and the underlying molecular requirements, Nat. Commun. 9 (2018) 4966, https://doi.org/10.1038/s41467-018-07450-0.

[30] A. Komuro, et al., WW domain-containing protein YAP associates with ErbB-4 and acts as a Co-transcriptional activator for the carboxyl-terminal fragment of ErbB-4 That translocates to the nucleus, J Biol Chem (2003), https://doi.org/10.1074/jbc.M305597200.

[31] M.V. Kuleshov, et al., Enrichr: a comprehensive gene set enrichment analysis web server 2016 update, Nucleic Acids Res. 44 (W1) (2016 Jul 8) W90–W97, https://doi.org/10.1093/nar/gkw377. Epub 2016 May 3.

[32] A. Karystinou, A.J. Roelofs, A. Nev, F.P. Cantator, H. Wackerhage, C. De Bari, Arthritis Res Ther. Nat Protoc. 17 (0) (2015 May 30) 147, https://doi.org/10.1186/s13075-015-0639-9.

[33] H.I. Chen, M. Sudol, The WW domain of Yes-associated protein binds a proline-rich ligand that differs from the consensus established for Src homology 3-binding modules, Proc Natl Acad Sci U S A 92 (17) (1995 Aug 15) 7819–7823, https://doi.org/10.1073/pnas.92.17.7819. PMID: 7644498; PMCID: PMC41237.

[34] Lian, et al., The role of YAP transcription coactivator in regulating stem cell self-renewal and differentiation, Genes Dev. 24 (2010) 1106–1118.

[35] Z. Liang, et al., Cultured cells and wing disc size of silkworm can be controlled by the hippo pathway, Open Biol. 8 (2018), 180029, https://doi.org/10.1098/rsob.180029.

[36] Z. Lin, Z. Yang, R. Xie, Z. Ji, K. Guan, M. Zhang, Decoding WW domain tandem-mediated target recognitions in tissue growth and cell polarity, Elife 8 (2019 Sep 5) e49439, https://doi.org/10.7554/eLife.49439. PMID: 31486770; PMCID: PMC6744271.

[37] Lorthongpanich, et al., YAP as a key regulator of adipo-osteogenic differentiation in human MSCs, Stem Cell Res Ther 10 (1) (2019 Dec 18) 402, https://doi.org/10.1186/s13287-019-1494-4.

[38] B.C. Low, C.Q. Pan, G.V. Shivashankar, A. Bershadsky, M. Sudol, M. Sheetz, YAP/TAZ as mechanosensors and mechanotransducers in regulating organ size and tumor growth, FEBS Lett. 588 (16) (2014 Aug 19) 2663–2670, https://doi.org/10.1016/j.febslet.2014.04.012. Epub 2014 Apr 18. (24747426).

[39] D. Mosqueira, S. Pagliari, K. Uto, M. Ebara, S. Romanazzo, C. Escobedo-Lucea, J. Nakanishi, A. Taniguchi, O. Franzese, P. Di Nardo, M.J. Goumans, E. Traversa, P. Pinto-do-Ó, T. Aoyagi, G. Forte, Hippo pathway effectors control cardiac progenitor cell fate by acting as dynamic sensors of substrate mechanics and nanostructure, ACS Nano 8 (3) (2014 Mar 25) 2033–2047, https://doi.org/10.1021/nn4058984.

[40] G. Nardone, J. Oliver-De La Cruz, J. Vrbsky, et al., YAP regulates cell mechanics by controlling focal adhesion assembly, Nat. Commun. 8 (2017), 15321, https://doi.org/10.1038/ncomms15321.

[41] K.H. Narsinh, et al., Comparison of human induced pluripotent and embryonic stem cells: Fraternal or identical twins? Mol. Ther. (2011) https://doi.org/10.1038/mt.2011.41.

[42] M.G. Noh, S.S. Kim, E.C. Hwang, D.D. Kwon, C. Choi, Yes-associated protein expression is correlated to the differentiation of prostate adenocarcinoma, J Pathol Transl Med. 51 (4) (2017) 365–373, https://doi.org/10.4132/jptm.2017.05.04.

[43] T. Oka, et al., Mst2 and lats kinases regulate apoptotic function of yes kinase-associated protein (YAP), J Biol Chem (2008), https://doi.org/10.1074/jbc.M804380200.

[44] T. Oka, M. Sudol, Nuclear localization and pro-apoptotic signaling of YAP2 require intact PDZ-binding motif, Genes Cells 14 (5) (2009 May) 607–615, https://doi.org/10.1111/j.1365-2443.2009.01292.x. Epub 2009 Apr 15. (19371381).

[45] J. Oliver-De La Cruz, G. Nardone, J. Vrbsky, A. Pompeiano, A.R. Perestrelo, F. Capradossi, K. Melajová, P. Filipensky, G. Forte, Substrate mechanics controls adipogenesis through YAP phosphorylation by dictating cell spreading, Biomaterials 205 (2019 Jun) 64–80, https://doi.org/10.1016/j.biomaterials.2019.03.009. Epub 2019 Mar 16. PMID: 30904599.
[46] Overholtzer, et al., Transforming properties of YAP, a candidate oncogene on the chromosome 11q22 amplicon, Proc. Natl. Acad. Sci. U. S. A. 103 (2006) 12405–12410.
[47] D. Pan, The hippo signaling pathway in development and cancer, Dev. Cell 19 (4) (2010 Oct 19) 491–505, https://doi.org/10.1016/j.devcel.2010.09.011. PMID: 20951342; PMCID: PMC3124840.
[48] H.W. Park, Y.C. Kim, B. Yu, T. Moroishi, J.-S. Mo, S.W. Plouffe, Z. Meng, K.C. Lin, F.-X. Yu, C.M. Alexander, C.-Y. Wang, K.-L. Guan, Alternative Wnt signaling activates YAP/TAZ, Cell 162 (2015) 780–794.
[49] T. Pawson, P. Nash, Assembly of cell regulatory systems through protein interaction domains, Science. 300 (5618) (2003 Apr 18) 445–452, https://doi.org/10.1126/science.1083653 (PMID: 12702867).
[50] S.W. Plouffe, A.W. Hong, K.L. Guan, Disease implications of the Hippo/YAP pathway, Trends Mol. Med. 21 (4) (2015 Apr) 212–222, https://doi.org/10.1016/j.molmed.2015.01.003. Epub 2015 Feb 18. PMID: 25702974; PMCID: PMC4385444.
[51] H. Qin, M. Hejna, Y. Liu, et al., YAP induces human naive Pluripotency, Cell Rep. 14 (10) (2016) 2301–2312, https://doi.org/10.1016/j.celrep.2016.02.036.
[52] A. Ramos, F.D. Camargo, The Hippo signaling pathway and stem cell biology, Trends Cell Biol. 22 (7) (2012 Jul) 339–346, https://doi.org/10.1016/j.tcb.2012.04.006. Epub 2012 May 31. PMID: 22658639; PMCID: PMC3383919.
[53] Sakabe, et al., Hippo signaling regulates vascular development, Proceed. Nat. Acad. Sci. (2017), https://doi.org/10.1073/pnas.1704030114, 201704030.
[54] M. Sudol, T. Hunter, NeW wrinkles for an old domain, Cell. 103 (7) (2000 Dec 22) 1001–1004, https://doi.org/10.1016/s0092-8674(00)00203-8 (11163176).
[55] X. Liu, N. Yang, S. Figel, et al., PTPN14 interacts with and negatively regulates the oncogenic function of YAP, Oncogene 32 (2013) 1266–1273, https://doi.org/10.1038/onc.2012.147.
[56] M. Sudol, YAP1 oncogene and its eight isoforms, Oncogene. 32 (33) (2013 Aug 15) 3922, https://doi.org/10.1038/onc.2012.520. Epub 2012 Nov 19. PMID: 23160371.
[57] M. Oren, Y. Aylon, The Hippo Signaling Pathway and Cancer, Springer, 2013, p. 354. Eur 160.45, ISBN: 978–1–4614-6219-4, https://doi.org/10.1007/978-1-4614-6220-0.
[58] R.N. Judson, A.M. Tremblay, P. Knopp, R.B. White, R. Urcia, C. De Bari, P. S. Zammait, F.D. Camargo, H. Wackerhage, The Hippo pathway member Yap plays a key role in influencing fate decisions in muscle satellite cells, J Cell Sci. 125(Pt 24) (2012 Dec 15) 6009–6019, https://doi.org/10.1242/jcs.109546. Epub 2012 Oct 4. PMID: 23038772; PMCID: PMC3585517.
[59] M. Sudol, P. Bork, A. Einbond, K. Kastury, T. Druck, M. Negrini, K. Huebner, D. Lehman, Characterization of the mammalian YAP (yes-associated protein) gene and its role in defining a novel protein module, the WW domain, J. Biol. Chem. 270 (24) (1995 Jun 16) 14733–14741, https://doi.org/10.1074/jbc.270.24.14733 (7782338).
[60] M. Sudol, Yes-associated protein (YAP65) is a Proline-Rich Phosphoprotein that binds to the SH3 domain of the yes proto-oncogene product, Oncogene 9 (1994) 2145–2152.
[61] M. Sudol, From Src homology domains to other signaling modules: proposal of the 'protein recognition code, Oncogene 17 (1998) 1469–1474.
[62] M. Sudol, K.F. Harvey, Modularity in the hippo signaling pathway, Trends Biochem. Sci. 35 (11) (2010 Nov) 627–633, https://doi.org/10.1016/j.tibs.2010.05.010. Epub 2010 Jul 2. (20598891).
[63] M. Sudol, YAP1 oncogene and its eight isoforms, Oncogene. 32 (33) (2013 Aug 15) 3922, https://doi.org/10.1038/onc.2012.520. Epub 2012 Nov 19. PMID: 23160371.
[64] D. Torre, A. Lachmann, A. Ma'ayan, BioJupies: automated generation of interactive notebooks for RNA-Seq data analysis in the cloud, Cell Systems 7 (5) (2018 Nov 28) 556–561, https://doi.org/10.1016/j.cels.2018.10.007, e3, Epub 2018 Nov 14, https://amp.pharm.mssm.edu/biojupies/dashboard.
[65] R. Tsutsumi, M. Masoudi, A. Takahashi, Y. Fujii, T. Hayashi, I. Kikuchi, Y. Satou, M. Taira, M. Hatakeyama, YAP and TAZ, hippo signaling targets, act as a rheostat for nuclear SHP2 function, Dev. Cell 26 (6) (2013 Sep 30) 658–665, https://doi.org/10.1016/j.devcel.2013.08.013. Epub 2013 Sep 12. (24035415).
[66] Varelas, et al., The Hippo pathway effectors TAZ and YAP in development, homeostasis and disease, Development 141 (2014) 1614–1626, https://doi.org/10.1242/dev.102376.
[67] A. Vassilev, K.J. Kaneko, H. Shu, Y. Zhao, M.L. DePamphilis, TEAD/TEF transcription factors utilize the activation domain of YAP65, a Src/yes-associated protein localized in the cytoplasm, Genes Dev. 15 (10) (2001) 1229–1241, https://doi.org/10.1101/gad.888601.
[68] D. Wennmann, B. Vollenbröker, A. Eckart, et al., The hippo pathway is controlled by angiotensin II signaling and its reactivation induces apoptosis in podocytes, Cell Death Dis. 5 (2014), e1519, https://doi.org/10.1038/cddis.2014.476.
[69] H. Zhang, M. Deo, R.C. Thompson, M.D. Uhler, D.L. Turner, Negative regulation of Yap dauring neuaronal differentiation, Dev Biol. 361 (1) (2012 Jan 1) 103–115, https://doi.org/10.1016/j.ydbio.2011.10.017. Epub 2011 Oct 18. PMID: 22037235; PMCID: PMC3235039.
[70] Yu-An, et al., WW domain-containing proteins YAP and TAZ in the hippo pathway as key regulators in Stemness maintenance, tissue homeostasis, and tumorigenesis, Front. Oncol. (2019), https://doi.org/10.3389/fonc.2019.00060.
[71] L. Zhang, F. Ren, Q. Zhang, Y. Chen, B. Wang, J. Jiang, The TEAD/TEF family of transcription factor Scalloped mediates Hippo signaling in organ size control, Dev. Cell 14 (3) (2008 Mar) 377–387, https://doi.org/10.1016/j.devcel.2008.01.006. Epub 2008 Feb 7. PMID: 18258485; PMCID: PMC2292673.
[72] Zhang, et al., The Merlin/NF2 tumor suppressor functions through the YAP oncoprotein to regulate tissue homeostasis in mammals, Dev. Cell 19 (2010) 27–38.
[73] Zhao, et al., Inactivation of YAP oncoprotein by the hippo pathway is involved in cell contact inhibition and tissue growth control, Genes Dev. (2007), https://doi.org/10.1101/gad.1602907.
[74] Zhao, et al., Both TEAD-binding and WW domains are required for the growth stimulation and oncogenic transformation activity of yes-associated protein, Cancer Res. (2009), https://doi.org/10.1158/0008-5472.CAN-08-2997.
[75] Zhou, et al., Mst1 and Mst2 protein kinases restrain intestinal stem cell proliferation and colonic tumorigenesis by inhibition of Yes-associated protein (Yap) overabundance, Proc. Natl. Acad. Sci. U. S. A. 108 (49) (2011) E1312–E1320.
[76] Qin, et al., YAP/TAZ Regulates TGF-β/Smad3 Signaling by Induction of Smad7 via AP-1 in Human Skin Dermal Fibroblasts, 2017, https://doi.org/10.1186/s12964-018-0232-3.
[77] T. Yamauchi, T. Moroishi, Hippo pathway in mammalian adaptive immune system, Cells. Apr 30 (5) (2019) 398, https://doi.org/10.3390/cells8050398. PMID: 31052239; PMCID: PMC6563119.
[78] H. Han, et al., TRRUST v2: An expanded reference database of human and mouse transcriptional regulatory interactions, Nucleic Acids Res. (2018), https://doi.org/10.1093/nar/gkx1013.
[79] R. Oughtred, et al., The BioGRID database: a comprehensive biomedical resource of curated protein, genetic, and chemical interactions, Protein Sci. (2021), https://doi.org/10.1002/pro.3978.
[80] S. Pagliari, et al., YAP-TEAD1 control of cytoskeleton dynamics and intracellular tension guides human pluripotent stem cell mesoderm specification, Cell Death Differ. (2020), https://doi.org/10.1038/s41418-020-00643-5.
[81] D. Szklarczyk, et al., STRING v11: protein-protein association networks with increased coverage, supporting functional discovery in genome-wide experimental datasets, Nucleic Acids Res. (2019), https://doi.org/10.1093/nar/gky1131.
[82] A.R. Perestrelo, et al., Multiscale analysis of extracellular matrix Remodeling in the failing heart, Circ. Res. (2021), https://doi.org/10.1161/CIRCRESAHA.120.317685.
[83] F. Zanconato, M. Forcato, G. Battilan, L. Azzolin, E. Quaranta, B. Bodega, A. Rosato, s. Bicciato, M. Cordenonsi, S. Piccolo, Genome-wide association between YAP/TAZ/TEAD and AP-1 at enhancers drives oncogenic growth, Nat Cell Biol. 17 (9) (2015 Sep) 1218–1227, https://doi.org/10.1038/ncb3216. Epub 2015 Aug 10. PMID: 26258633; PMCID: PMC6186417.
[84] F. Martino, A.R. Perestrelo, V. Vinarský, S. Pagliari, G. Forte, Cellular Mechanotransduction: From Tension to Function, Front Physiol. 9 (2018 Jul 5) 824, https://doi.org/10.3389/fphys.2018.00824. PMID: 30026699; PMCID: PMC6041413.